

RESEARCH

Open Access



Spatial patterns and temporal trends of trace elements in mosses from 1990 to 2020 in Germany

Winfried Schröder^{1*}, Stefan Nickel², Annekatriin Dreyer³ and Barbara Völksen²

Abstract

Background The accumulation of trace elements in mosses is used as an indirect measure of atmospheric deposition and an important complement to the techniques used to monitor the Geneva Air Pollution Convention. The aim of this paper is to quantify and map temporal and spatial trends of metal enrichment in mosses collected in Germany in 1990, 1995, 2000, 2005, 2015 and 2020. Collection and chemical analysis of the moss samples were carried out according to international guidelines.

Results The analysis shows that since 1990, the median concentrations of As, Cd, Cu, Ni, Pb and Sb in the mosses have been decreasing significantly, with the highest decline of Pb (− 86%). This trend reversed in 2000 and 2005 and between 2015 and 2020 by increases in the concentrations of some trace elements. In the 2000 Moss Survey, higher concentrations were measured for Cd, Cu, Ni and Sb than in 2015, ranging from + 26% (Cu) to + 165% (Ni). For As and Pb, no significant changes can be observed in 2020 compared to 2015. The increase in metal concentrations in the mosses over the last five years does not correspond to the corresponding trends in reported metal emissions in Germany (2015–2020). In contrast, the long-term trends of the As, Cd, Cu, Ni and Pb concentrations measured in the mosses showed good overall correspondence with the emission trends in Germany (1990–2020). The long-term trends of the moss data are mostly weaker than those of the emission data. The spatial patterns of the temporal trends were mapped and discussed for As, Cd, Cu, Ni, Pb and Sb.

Conclusions The study shows that for valid monitoring of atmospheric deposition, it is not enough to consider only emission data or the modelled deposition derived from these data. In this respect, the study provides one of many necessary contributions to the discussion on the extent to which analytes of current monitoring programmes are still relevant and up-to-date and whether there are new substances that are also relevant or even more relevant than existing analytes and to what extent this should be taken into account in designing future environmental monitoring.

Keywords Deposition, Emission, Geostatistics, *Hypnum cupressiforme*, *Pleurozium schreberi*, *Pseudoscleropodium purum*, Percentile statistics

*Correspondence:

Winfried Schröder
winfried.schroeder@uni-vechta.de

¹ Chair of Landscape Ecology, University of Vechta, P.O. Box 155, 49364 Vechta, Germany

² Office for Ecological Planning, PlanWerk, Unterdorfstraße 3, 63667 Nidda, Germany

³ ANECO Institute for Environmental Protection GmbH & Co, Großmoorkehre 4, 21079 Hamburg, Germany

Background and aim

The International Moss Survey, which has been conducted every five years since 1990, serves as a Europe-wide review of the objectives of the 1979 Geneva

Convention on Long-Range Transboundary Air Pollution [1, 2]. Chemical analysis includes trace elements¹ (since 1990), nitrogen (since 2005), persistent organic pollutants (since 2010) and microplastics (since 2020) at up to 7312 sites in Europe. In Germany, 592 sites were sampled in 1990 [6], 1026 in 1995 [7, 8], 1028 in 2000 [9], 726 in 2005 [10], 400 in 2015 [11] and 26 in 2020. Germany did not take part in the 5th moss survey carried out in 2010. This research is to combine the metal contents measured in the 2020 survey with those from all previous campaigns, to analyze and map them geostatistically, and to update the temporal trends in metal enrichment for the years 1990–2020.

Material and methodology

Sampling and analysis

The reduction of sampling sites from 400 (Moss Monitoring 2015, MM2015 in short) to 26 (MM2020) was based on decision modelling, neighbourhood and inferential statistics aiming at minimizing bias and loss of information [12, 13]. The sampling of moss species *Hypnum cupressiforme*, *Pleurozium schreberi* and *Pseudoscleropodium purum* as well as their preparation and chemical analysis of the trace elements were carried out according to international guidelines [2], as in all moss surveys. From 2 to 7 (on average 5) subsamples were collected from each moss sampling site. The moss samples for the determination of trace elements were taken using PE gloves in the period from the end of August to the beginning of October 2021, stored in 1L LDPE ziplock bags (Topitz company) and sent to the laboratory (ANECO Institut für Umweltschutz GmbH & Co) after sampling. The receipt of the samples was documented, the samples were labelled with sample numbers and stored in the dark at approx. 8 °C in the refrigerator until further preparation. The preparation of the moss samples was carried out according to the ICP Vegetation [2] by four persons within two weeks after the arrival of the samples. The moss samples were only touched with PE gloves. The samples were cleaned of adhering foreign material (e.g., grass, needles, leaves, soil particles.). The moss samples were not washed. Green and green–yellow moss shoots were separated from the rest of the sample using cleaned ceramic scissors and Teflon tweezers. The quality of the preparation was checked continuously, i.e., the sample material separated for chemical analyses was continuously visually checked by the person handling the sample as well as, after finishing the preparation, by a second person (4-eyes principle). Furthermore, the cleanliness and adequate usage of equipment was regularly

inspected. After sample preparation, the moss samples were analyzed.

The content of moss dry substance was determined after drying at 105 °C.

For element analysis, the moss samples were dried at 60 °C and ground to a homogeneous fine powder (Retsch SM 200, tungsten carbide coated insert, 20 s. at 10.000 rpm followed by a Pulverisette 14 (Fritsch) equipped with a 0.5 mm Reintitan sieve at 20.000 rpm). For the analysis of the elements Al, As, Cd, Cr, Cu, Fe, Ni, Pb, Sb, V, Zn and Hg, approx. 0.5 g of the dried moss samples were digested by microwave-assisted pressure digestion (microwave Mars Xpress CEM samt) with 5 ml 65% nitric acid and 1 ml 30% hydrogen peroxide after a pre-reaction of approx. 1 h at a maximum of 1800 W and a constant temperature of 200 °C (heating phase to 200° in 20 min, 200 °C for 18 min). The determination of Al, As, Cd, Cr, Cu, Fe, Ni, Pb, Sb, V and Zn was performed according to DIN EN ISO 17294-2 (ISO 2017) by an ICP-MS (Agilent 7900 with sample loop). Mercury was analyzed according to DIN ISO 16772 (2005-06) by cold vapour AAS (Mercur) after reduction with tin(II) chloride without enrichment.

A blank sample and moss reference material (moss standards M2 and M3 characterized by [14]) were digested with the sample series to check element recoveries and thus infer on analytical performance. The moss standard samples consisted of residual material from the 2015 moss monitoring, which had been stored at room temperature in the dark in PE centrifuge tubes.

Statistical analysis

The statistical evaluation of the data on metal concentrations in the mosses largely corresponds to the methods used for the nitrogen concentrations not considered in this article. They were described in more detail by Nickel et al. [15] than is possible here. First, the statistical distribution of the metal concentrations in the moss samples was determined (outliers, minimum, maximum, mean, standard deviation, relative coefficient of variation as well as 20th, 50th, 90th, 98th percentile). For the graphical analysis of the substance concentrations and their temporal trends, the relative heights of the element-specific annual medians of all six monitoring campaigns (1990, 1995, 2000, 2005, 2015 and 2020) were calculated in relation to the corresponding element-specific overall median of all values from 1990 to 2020 according to Eq. 1. The median was preferred to the mean value, as it is more robust in the case of asymmetrical distributions and in the face of outliers.

Relative level of annual median [% of total median 1990–2020].

¹ For terminology, refer to Hodson [3], Pourret [4] and Vernon [5].

Table 1 Results of the measurement quality assurance

Element (in reference sample)	M2		M3	
	Actual value mg/kg	Target value mg/kg	Actual value mg/kg	Target value mg/kg
Aluminium (Al)	192	178 ± 15	173	169 ± 10
Arsenic (As)	1.05	0.98 ± 0.07	0.10	0.105 ± 0.007
Cadmium (Cd)	0.455	0.454 ± 0.019	0.106	0.106 ± 0.005
Chromium (Cr)	1.03	0.97 ± 0.17	0.72	0.67 ± 0.19
Copper (Cu)	68.8	68.7 ± 2.5	4.0	3.76 ± 0.23
Iron (Fe)	226	262 ± 35	150	138 ± 12
Nickel (Ni)	16.4	16.3 ± 0.9	0.9	0.95 ± 0.08
Lead (Pb)	5.46	6.37 ± 0.43	3.46	3.33 ± 0.25
Antimony (Sb)	0.20	0.21 ± 0.016	0.059	0.052 ± 0.007
Vanadium (V)	1.54	1.43 ± 0.17	1.11	1.19 ± 0.15
Zinc (Zn)	36.1	36.1 ± 1.2	26.2	25.4 ± 1.1
Mercury (Hg)	0.091	0.058 ± 0.005	0.060	0.035 ± 0.004

$$\text{Conc}_{\text{median}} = \frac{\text{Conc}_{\text{annual median}}}{\text{Conc}_{\text{total median}}} * 100 \quad (1)$$

To quantify the trends and to provide inferential statistical support, the changes in the median values [%] were calculated for the six monitoring campaigns and a two-sided Mann–Whitney U test [16] was carried out in each case. The calculations were made for the paired campaign combinations 1990/1995, 1995/2000, 2000/2005, 2005/2015 and 2015/2020, i.e., in each case by comparison with the previous campaign. Secondly, the changes in the median values were calculated in relation to the base year, i.e., the year in which the respective measured values were determined for the first time. In both cases, the median from the respective previous campaign was set equal to 100%.

To investigate whether and to what extent the number of sample elements in the MM2020 is sufficient for the inferential statistical trend analysis, selected percentiles (20th, 50th, 90th percentile) of the series of measurements on trace elements of the total sample (= depending on the element, from 397 to 400 sites of the MM 2015) were compared with those of the respective subsample (= 26 sites of the MM2015, which were also sampled in the MM2020 within a radius of 2 km). For the statistical distributions of trace elements, a two-sided inferential statistical comparison was performed using the Mann–Whitney U -test and checked whether the two independent samples originate from the same population. Items with significant differences in the measured value distributions of the full and partial sample of the MM2015 ($p < 0.1$) were—under the assumption that they behave

the same way to each other in the MM2020—excluded from further consideration.

Geostatistical methods [17] were used to map the spatial patterns of metal accumulation. Such methods are based on the theory of regionalised variables [18]. According to this theory, spatial interpolations between spatially discrete sampling or measurement locations are only meaningful if the measured values of closely spaced locations are more similar than values of more distant locations. Only if such spatial autocorrelations of the measured values can be proven, the further use of the data set for area estimates with Kriging interpolation makes sense.

The existence of spatial autocorrelation was checked by means of variogram analysis [19]. For this purpose, the distance between spatially located pairs of points is related to the similarity of the measured values at these points in an experimental semi-variogram (abbreviated as “variogram” and a suitable model variogram (= variogram curve) is fitted to it. From the model variogram, the following characteristic values can be derived to describe the spatial autocorrelation: The *nugget effect* provides information about the spatial variability below the smallest measuring point distance. The *range* quantifies the maximum spatial distance within which a dependency between *distance* and *semivariance* is recognisable and thus the interpolation can be regarded as statistically meaningful. The *semivariance* assigned to the *range* is called the *sill*. The higher the *nugget/sill ratio* in %, the lower the spatial autocorrelation. If this ratio approaches 100%, there is no spatial autocorrelation. The prerequisite for using the model

Table 2 Metal concentrations in moss samples (MM2020)

Monitoring site	Moss species	Aluminium (Al) mg/kg	Arsenic (As) mg/kg	Cadmium (Cd) mg/kg	Chromium (Cr) mg/kg	Copper (Cu) mg/kg	Iron (Fe) mg/kg	Nickel (Ni) mg/kg	Lead (Pb) mg/kg	Antimony (Sb) mg/kg	Vanadium (V) mg/kg	Zinc (Zn) mg/kg	Mercury (Hg) mg/kg
BB119_1	<i>Plesch</i>	162	0.08	0.16	0.64	4.85	153	0.87	0.93	0.16	0.34	27.3	0.112
BW980_1	<i>Hypcup</i>	596	0.12	0.29	1.42	6.11	468	2.36	3.24	0.19	1.00	58.5	0.154
BY206	<i>Hypcup</i>	248	0.08	0.37	1.02	4.36	236	1.95	1.29	0.15	0.41	68.5	0.265
BY227_1	<i>Plesch</i>	261	0.08	0.14	1.05	3.93	203	1.63	0.96	0.12	0.49	18.9	0.126
BY228_1	<i>Plesch</i>	386	0.10	0.12	1.22	4.41	299	1.96	1.41	0.18	0.59	24.9	0.165
HE64	<i>Hypcup</i>	563	0.10	0.18	2.92	4.88	518	3.98	2.94	0.10	1.20	24.6	0.060
MV114_2	<i>Psepur</i>	267	0.12	0.29	1.02	6.21	291	1.33	1.48	0.15	0.71	46.1	0.124
NI124_139	<i>Plesch</i>	306	0.12	0.13	1.63	4.55	343	1.86	2.02	0.21	1.42	26.4	0.170
NI03_95	<i>Plesch</i>	146	0.08	0.19	0.82	7.44	198	0.97	1.19	0.15	0.71	37.1	0.044
NI86_1	<i>Plesch</i>	319	0.15	0.21	1.24	5.87	321	1.26	1.60	0.16	0.75	42.7	0.172
NI104_88	<i>Psepur</i>	110	0.05	0.13	0.79	5.08	177	0.64	0.94	0.12	0.60	36.2	0.021
NI108_98	<i>Psepur</i>	97	0.03	0.14	0.78	4.27	88	0.78	0.61	0.12	0.26	36.7	0.048
NI116_123	<i>Plesch</i>	348	0.13	0.17	1.98	7.97	359	2.10	3.02	0.13	1.12	37.0	0.080
NI117_124	<i>Psepur</i>	194	0.11	0.22	1.32	14.50	282	1.29	1.77	0.16	1.02	80.4	0.120
NI118_128	<i>Psepur</i>	244	0.06	0.11	1.28	5.87	259	1.26	1.37	0.13	0.67	45.6	0.051
NI130_157	<i>Plesch</i>	139	0.05	0.07	0.80	5.87	91	0.83	0.75	0.11	0.32	33.4	0.031
NW27	<i>Hypcup</i>	646	0.25	0.40	3.28	7.57	547	4.77	7.91	0.39	1.25	83.6	0.090
NW39	<i>Hypcup</i>	360	0.13	0.21	1.76	5.32	356	2.12	5.56	0.22	0.92	27.9	0.067
RP27	<i>Psepur</i>	491	0.18	0.20	1.73	5.19	265	2.93	1.07	0.08	0.66	33.9	0.053
SH36_2	<i>Psepur</i>	173	0.08	0.24	0.80	8.88	223	1.60	1.98	0.13	0.54	53.4	0.436
SL5	<i>Psepur</i>	331	0.23	0.29	2.97	6.04	425	1.90	4.76	0.11	1.22	57.1	0.169
SL9_2	<i>Hypcup</i>	595	0.22	0.34	4.69	5.98	749	3.64	11.18	0.16	1.87	59.1	0.174
SN240_1	<i>Hypcup</i>	908	0.32	0.23	2.83	6.07	1544	5.02	3.69	0.17	1.48	24.9	0.135
ST199_1	<i>Psepur</i>	335	0.12	0.29	1.17	7.09	317	1.74	2.20	0.13	0.60	45.5	0.137
ST204_1	<i>Plesch</i>	410	0.25	0.34	1.47	6.70	492	1.73	8.17	0.22	0.90	73.5	0.191
TH68	<i>Hypcup</i>	426	0.15	0.22	1.41	5.23	360	2.50	3.77	0.22	0.90	39.1	0.116

Bold outlier values*Plesch* *Pleurozium schreberi*, *Psepur* *Pseudoscleropodium purum*, *Hypcup* *Hypnum cupressiforme*

Table 3 Descriptive-statistical characteristics of metal concentrations in moss samples and geostatistical area estimates (the latter in brackets), MM2020

Element	<i>n</i>	Min [μg/g]	P ₂₀ [μg/g]	P ₅₀ [μg/g]	P ₉₀ [μg/g]	P ₉₈ [μg/g]	Max [μg/g]	MW [μg/g]	SD [μg/g]	CV [%]
Al	26	96.7	173.0	325.1	595.5	777.1	908.4	348.5	193.4	55.5
As	26 (39,744)	0.027 (0.030)	0.079 (0.103)	0.119 (0.133)	0.240 (0.203)	0.287 (0.235)	0.322 (0.315)	0.131 (0.139)	0.073 (0.043)	55.6 (31.2)
Cd	26 (39,744)	0.073 (0.102)	0.138 (0.193)	0.210 (0.225)	0.341 (0.292)	0.384 (0.333)	0.396 (0.374)	0.218 (0.228)	0.086 (0.045)	39.3 (19.7)
Cr	26	0.641	0.816	1.300	2.944	3.982	4.687	1.616	0.969	60.0
Cu	26 (39,744)	3.93 (3.94)	4.85 (4.92)	5.87 (5.62)	7.77 (6.82)	11.69 (7.92)	14.50 (8.85)	6.16 (5.69)	2.10 (0.86)	34.0 (15.2)
Fe	26	88.2	203.3	308.0	532.5	1146.3	1544.1	367.9	282.1	76.7
Hg	26	0.0206	0.0528	0.1222	0.1824	0.3504	0.4361	0.1273	0.0862	67.7
Ni	26 (39,744)	0.640 (1.053)	1.256 (1.348)	1.800 (2.264)	3.811 (3.060)	4.892 (3.375)	5.016 (3.493)	2.038 (2.194)	1.169 (0.669)	57.4 (30.5)
Pb	26 39,744	0.61 (0.91)	1.07 (1.75)	1.88 2.4546	6.73 (4.42)	9.68 (5.63)	11.18 (7.07)	2.92 (2.72)	2.65 (1.14)	90.8 (41.8)
Sb	26 (39,744)	0.080 (0.101)	0.122 (0.144)	0.148 (0.160)	0.217 (0.191)	0.304 (0.247)	0.388 (0.294)	0.160 (0.163)	0.060 (0.026)	37.3 (16.3)
V	26	0.262	0.538	0.730	1.335	1.674	1.866	0.844	0.397	47.0
Zn	26	18.9	27.3	38.1	71.0	82.0	83.6	43.9	18.0	41.0

In parentheses: Characteristic values of the geostatistical area estimates

n sample size, P₂₀ 20th percentile, P₅₀ 50th percentile, P₉₀ 90th percentile, P₉₈ 98th percentile, MW arithmetic mean, SD standard deviation, CV relative coefficient of variation

Table 4 Percentile and *U* test statistics for the total sample 2015 (*n* = 397 to 400) and the sub-sample 2020 with concentration values of the year 2015 (*n* = 25)

Element	<i>n</i> (2015) [μg/g]	P ₂₀ (2015) [μg/g]	P ₅₀ (2015) [μg/g]	P ₉₀ (2015) [μg/g]	<i>n</i> (2020) [μg/g]	P ₂₀ (2020) [μg/g]	P ₅₀ (2020) [μg/g]	P ₉₀ (2020) [μg/g]	<i>p</i> -value (<i>U</i> test)
Al	400	138.88	196.9	460.84	25	173.1	270.1	493.04	0.06*
As	398	0.07	0.11	0.22	25	0.08	0.13	0.22	0.49
Cd	398	0.09	0.14	0.26	25	0.1	0.13	0.27	0.92
Cr	399	0.4	0.57	1.24	25	0.47	0.76	1.41	0.07*
Cu	400	3.55	4.65	7.77	25	3.26	4.81	6.98	0.50
Fe	400	152.12	206.15	433.02	25	181.04	250.4	534.46	0.04**
Hg	397	0.02	0.03	0.05	25	0.02	0.03	0.07	0.26
Ni	400	0.44	0.68	1.46	25	0.42	0.67	1.63	0.93
Pb	400	1.23	1.83	4.33	25	1.03	2.09	5.71	0.56
Sb	397	0.06	0.09	0.16	25	0.05	0.1	0.15	0.74
V	400	0.37	0.52	1.08	25	0.48	0.72	1.4	0.01***
Zn	400	22.68	30.69	48.21	25	27.45	35.43	51.09	0.08*

n number of values above the limit of quantification (BG); values < BG were not considered for the characteristic value calculations, P₂₀ 20th percentile, P₅₀ 50th percentile, P₉₀ 90th percentile

****p* ≤ 0.01 (very significant)

***p* ≤ 0.05 (significant)

**p* ≤ 0.1 (weakly significant)

variogram for kriging interpolation is generally *nugget/sill ratios* < 75%.

The Morans I statistic [20] was used to statistically test whether the spatial pattern formed by a group of objects (e.g., moss sites) is randomly distributed or

Table 5 Median values of metal concentrations in mosses 1990 to 2020

Element	Unit	1990 (n=475 to 592)	1995 (n=1026 to 1028)	2000 (n=1026 to 1028)	2005 (n=724 to 726)	2015 (n=397 to 400)	2020 (n=26)
As	µg/g	0.338	0.249	0.160	0.160	0.108 (0.101–0.114)	0.119 (0.082–0.135)
Cd	µg/g	0.287	0.293	0.210	0.210	0.136 (0.130–0.148)	0.210 (0.158–0.244)
Cu	µg/g	8.79	9.45	7.14	7.27	4.65 (4.44–4.84)	5.87 (5.08–6.11)
Ni	µg/g	2.353	1.630	1.130	1.160	0.681 (0.653–0.722)	1.800 (1.291–2.095)
Pb	µg/g	12.94	7.78	4.62	3.69	1.83 (1.69–1.97)	1.88 (1.29–3.02)
Sb	µg/g	n.a	0.173	0.150	0.160	0.090 (0.085–0.097)	0.148 (0.130–0.165)

In brackets: 95% confidence interval for the median value
n sample size, n.a. not specified

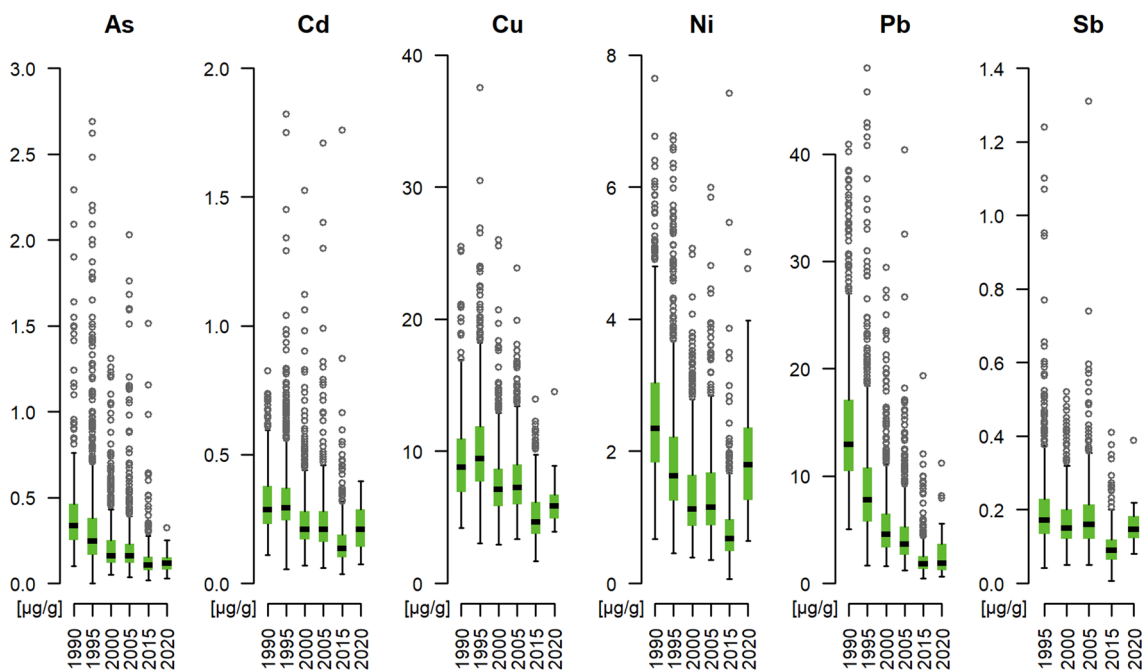


Fig. 1 Temporal trends of metal concentrations in moss samples 1990–2020

spatially grouped (“clustered”). Positive Morans I index values indicate a tendency to cluster and negative values indicate a tendency to scatter. Error probabilities of $p < 0.05$ mean that the measured values are not randomly distributed, i.e., the detected spatial autocorrelation is significant.

Following the detection of spatial autocorrelation by variogram analysis and Moran’s I-statistics and the selection of a suitable model variogram, the spatial patterns estimated by kriging interpolation were mapped. The quality of the estimation results obtained from kriging

was cross-validated [21]. In this process, one value each was taken in turn from the total set of measured values and re-estimated by kriging with the selected model variogram. The difference between the estimated value Z and the measured value z forms the experimental error ε [19]. The mean error (ME) and the mean standardised error (MSE) indicate over- or underestimation tendencies of the model variogram. The ME is calculated from the average deviations between measured and estimated values, the MSE relates the experimental error to the standard deviation SD. Both measures are ideally 0. The

Table 6 Changes in the median values of the metal concentrations to the previous campaign and to the previous-previous campaign [in %]

Element	1995/1990	2000/1995	2005/2000	2015/2005	2020/2015	1995/B. year	2000/B. year	2005/B. year	2015/B. year	2020/B. year
As	-26***	-36***	0	-32***	10	-26**	-53***	-53***	-68***	-65***
Cd	2	-28***	0	-35***	55***	2	-27***	-27***	-53***	-27***
Cu	8***	-24***	2**	-36***	26***	8**	-19***	-17***	-47***	-33***
Ni	-31***	-31***	3	-41***	165***	-31**	-52***	-51***	-71***	-23***
Pb	-40***	-41***	-20***	-50***	2	-40**	-64***	-71***	-86***	-86***
Sb	n.a	-13***	7**	-44***	64***	n.a	-13***	-8***	-48***	-14**

B. year-base year (year of first sampling), n.a. not specified, - decrease in median

***p ≤ 0.01 (very significant)

**p ≤ 0.05 (significant)

Table 7 Estimation method and model parameters

Element	<i>n</i>	<i>Vk</i>	<i>Sk</i>	Method	Transformation	lambda	Model	Lag size	No of lags	Sector type	Max. neighbours	Range
As	26	55.61	0.91	Ordinary	Log	–	Exponential	40,000	15	4 (45° offset)	10	305
Cd	26	39.30	0.38	Ordinary	–	–	Spherical	25,000	18	4 (45° offset)	10	228
Cu	19	21.39	0.73	Ordinary	–	–	Spherical	55,000	12	4 (45° offset)	10	271
Ni	26	57.36	1.15	Ordinary	Log	–	Spherical	42,000	18	4 (45° offset)	10	386
Pb	26	90.83	1.62	Ordinary	Log	–	Spherical	20,000	18	4 (45° offset)	10	137
Sb	26	37.26	2.03	Ordinary	Log	–	Spherical	12,000	36	4 (45° offset)	10	224

n sample size, *Vk* relative coefficient of variation [%], *Sk* skewness, *Method* Kriging method, *transformation Method* for transforming the target variable (* = significant); *lambda* Parameter of the Box-Cox transformation, *Model* Variogram model used, *Lag size* Size of the distance classes, *No of Lags* Number of distance classes, *Sector type* Neighbourhood parameter for splitting the search window, *Max. Neighbors* Maximum number of sample sites in the search window, *Range* Range of the spatial autocorrelation [km]

Table 8 Goodness measures of the geostatistical models and the area estimates

Analyst	Nugget	Partial Sill	N/S	Moran's I	<i>p</i> -value	ME	MSE	RMSSE	MPE	SR	MPEc	<i>r_p</i>
As	0.00	0.01	0.00	0.03	0.14	0	0.04	1.15	7.29	1.1	8	0.43
Cd	0.00	0.01	0.11	0.03	0.32	– 0.01	– 0.05	1.12	1.45	0.95	1.38	0.26
Cu	0.00	1.57	0.00	– 0.05	0.91	– 0.05	– 0.03	1.12	5.35	1	5.35	0.21
Ni	0.14	0.19	0.42	0.02	0.06	0.07	0.03	0.91	19.35	1.06	20.56	0.51
Pb	0.16	0.41	0.28	0.08	0.24	0.06	– 0.05	0.85	25.46	1.01	25.65	0.38
Sb	0.03	0.10	0.25	– 0.15	0.08	0	– 0.1	1.31	3.85	1.16	4.47	– 0.45

Nugget nugget, *Partial Sill* partial sill, *N/S* nugget/sill ratio, *Moran's I* Moran coefficient, *p-value* error probability for the Moran coefficient, *ME* mean error [µg/g or % Tr.], *MSE* mean standardised error, *RMSSE* variance of the root-mean-square standardised error, *MPE* median percentage error [%], *SR* Range Ratio ratio of range cross-validation error to range measured values, *MPEc* MPE multiplied by the range ratio [%], *r_p* Pearson's correlation coefficient

root mean square standardised error (RMSSE) reflects the relationship between experimental and theoretical variances and is ideally 1. An RMSSE smaller than 1 indicates an underestimation, larger than 1 an overestimation of the variance of the estimated values. The calculation of the Median of Percental Errors (MPE) serves to compare several measured variables with different scale expansions. If the cross-validation errors show a lower range than the empirical measured values, this speaks for the quality of the estimation model. One way to take this into account when calculating the estimation quality measure is to multiply the ratio between error ranges and empirical ranges (SR—range ratio) by the MPE. Another quality indicator is the correlation coefficient between measurement and estimation results. Ideally, this is 1 [22].

Variogram analyses and mapping of kriging area estimates were carried out using Geostatistical Analyst for ESRI ArcGIS 10.2. To illustrate the temporal evolution of areal patterns of metal content since MM1990, maps of MM2020 were contrasted with those of the 1990, 1995, 2000, 2005 and 2015 campaigns using the following measured value classifications:

1. Element-specific classification [2] according to previous reports for better comparability.

2. Element- and campaign-specific quantiles (10 percentile classes: up to 10th percentile, > 10th to 20th percentile, ... > 90th to 100th percentile, determined in each case on the basis of the measured values of the individual campaigns), which alone are intended to illustrate the spatial differentiation in the case of decreasing inputs, i.e., to enable statements to be made, for example, as to whether hot spots of earlier campaigns remain hot spots even with decreasing inputs, or whether the exposure patterns shift.
3. Element-specific and cross-campaign quantiles (10 percentile classes: 0 to 10th percentile, > 10th to 20th percentile, ... > 90th to 100th percentile, determined in each case on the basis of the available measured values of all campaigns), which allow a high and statistically meaningful degree of spatial and temporal differentiation in the case of declining element concentrations.

Results

Quality assurance

The results of the chemical-analytical quality assurance data (Table 1) revealed the recoveries for the trace elements other than mercury ranged between 86% (Fe) and 108% (Al) for M2 and between 93% (Ni) and 113% (Sb)

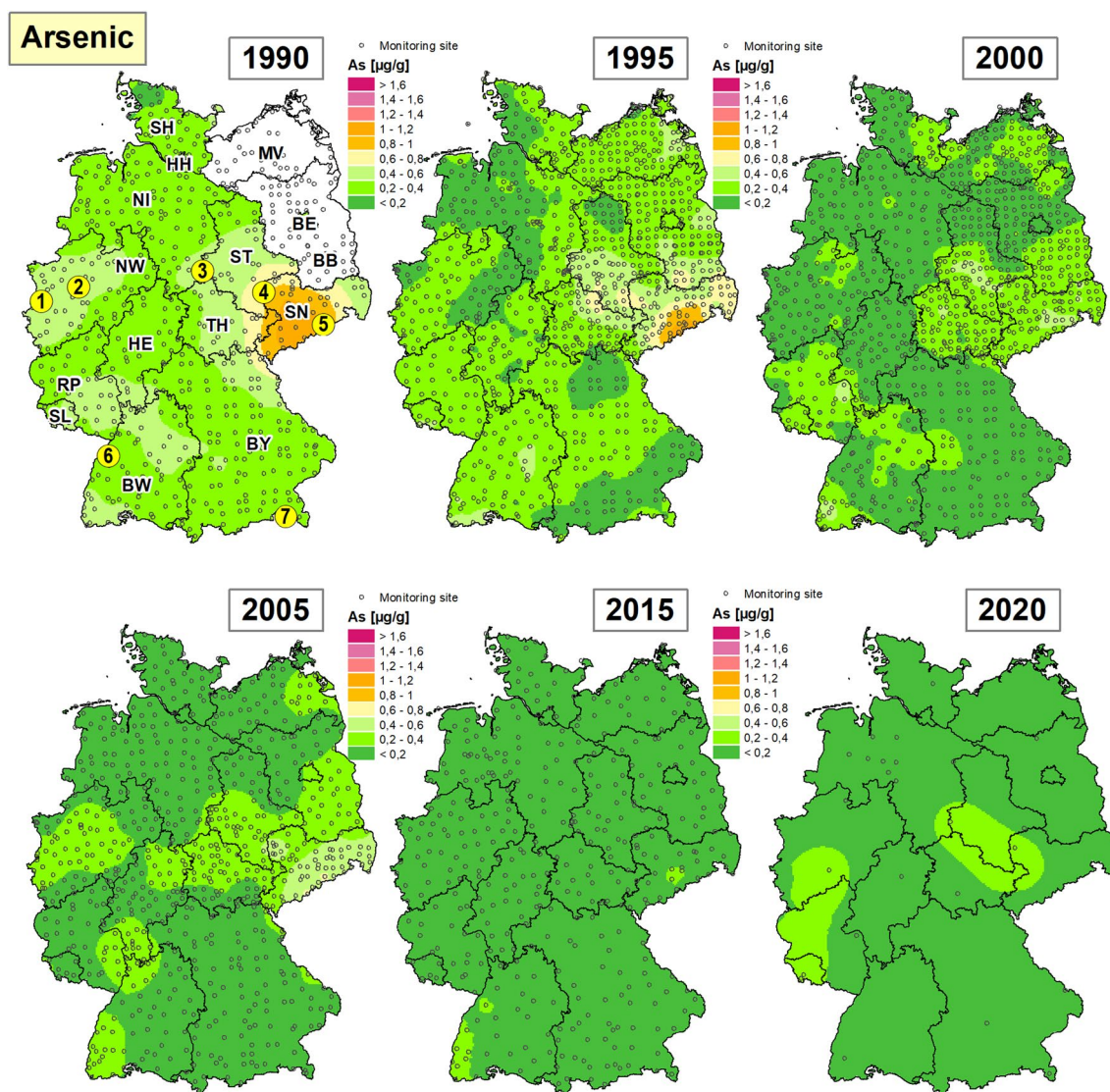


Fig. 2 Geostatistical time series of As concentrations (1990–2020) in mosses (measured value classification according to ICP Vegetation [2]). SH Schleswig–Holstein, HH Hamburg, NI Lower Saxony/Bremen, MV Mecklenburg–Western Pomerania, NW North-Rhine Westphalia, ST Saxony-Anhalt, BE Berlin, SL Saarland, RP Rhineland–Palatinate, HE Hesse, TH Thuringia, SN Saxony, BW Baden-Wuerttemberg, BY Bavaria. 1 Lower Rhine 2 Ruhr area 3 Harz Mountains 4 Halle/Leipzig area 5 Ore Mountains 6 Northern Upper Rhine 7 Alpine region

for M3. The recoveries for Hg reached 158% (M2) and 157 and 171% (M3). The overestimate data of Hg could not be explained, but could be due to the sample storage of the moss standard.

Measured values and their statistical distribution

Table 2 contains the measurement results, and Table 3 describes their statistical distribution and that of the geostatistical area estimates. The inferential statistical comparison of the distributions in the overall MM2015 monitoring network ($n = 397$ to 400) with the 2015 measurements at the MM2015 sites that were also sampled

in 2020 ($n = 25$)², shows significant differences ($p < 0.1$) in the 2015 measurement series for Al, Cr, Fe, V and Zn (Table 4). For example, the median value of Al concentrations at all 400 sites of MM2015 is 196.9 µg/g and in the sub-measurement network of MM2020 270.1 µg/g each with the values of MM2015, whereby the differences are to be classified as (weakly) significant (Table 4). In the following, therefore, only those trace elements are considered which do not show any significant differences between the distributions of the full and partial

² One site was sampled for the first time in MM2020, so only 25 of the 26 sites were available for comparison.

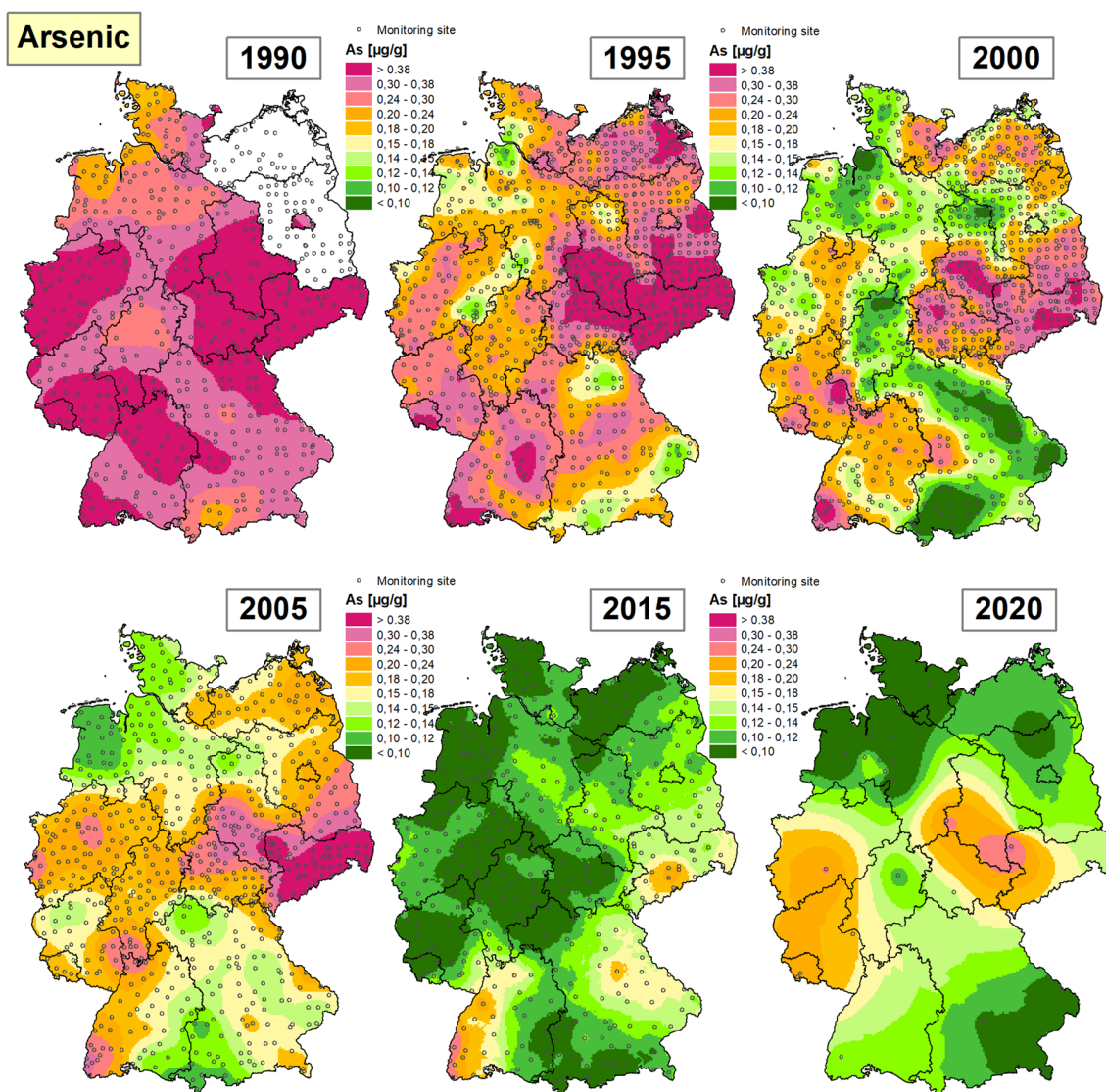


Fig. 3 Geostatistical time series of As concentrations (1990–2020) in mosses (cross-campaign percentile classes)

samples and for which it can thus be assumed that the 2020 monitoring network represents the concentrations in the moss similarly to the 2015 monitoring network. The result of the quality assurance was furthermore that the moss standards [14] were overestimated by 50% (M2) to 100% (M3) for Hg (Table 1), although the reason for this is unclear. The following site- and area-related trend analyses are, therefore, limited to the following 6 of the 12 trace elements investigated: As, Cd, Cu, Ni, Pb, Sb.

Spatial and temporal trends in metal concentrations in mosses

As—arsenic In MM2020. As concentrations between 0.027 and 0.322 µg/g were quantitatively determined in

mosses at a total of 26 sites in Germany (Table 2), with the highest value measured in Saxony in the Leipzig area (SN240_1). Other sites with As accumulations above the 90th percentile (0.240 µg/g) are found in Saxony-Anhalt and in North Rhine-Westphalia (Table 3). The target values of the M2 and M3 reference standards were met (Table 1).

The median value is 0.119 µg/g (Table 5) and thus lies approximately in the trend of the last monitoring campaigns (Fig. 1). Compared to MM2015, there is at least no significant increase in the As median (Table 6). The long-term trend since 1990 is clearly decreasing nationwide with – 65%.

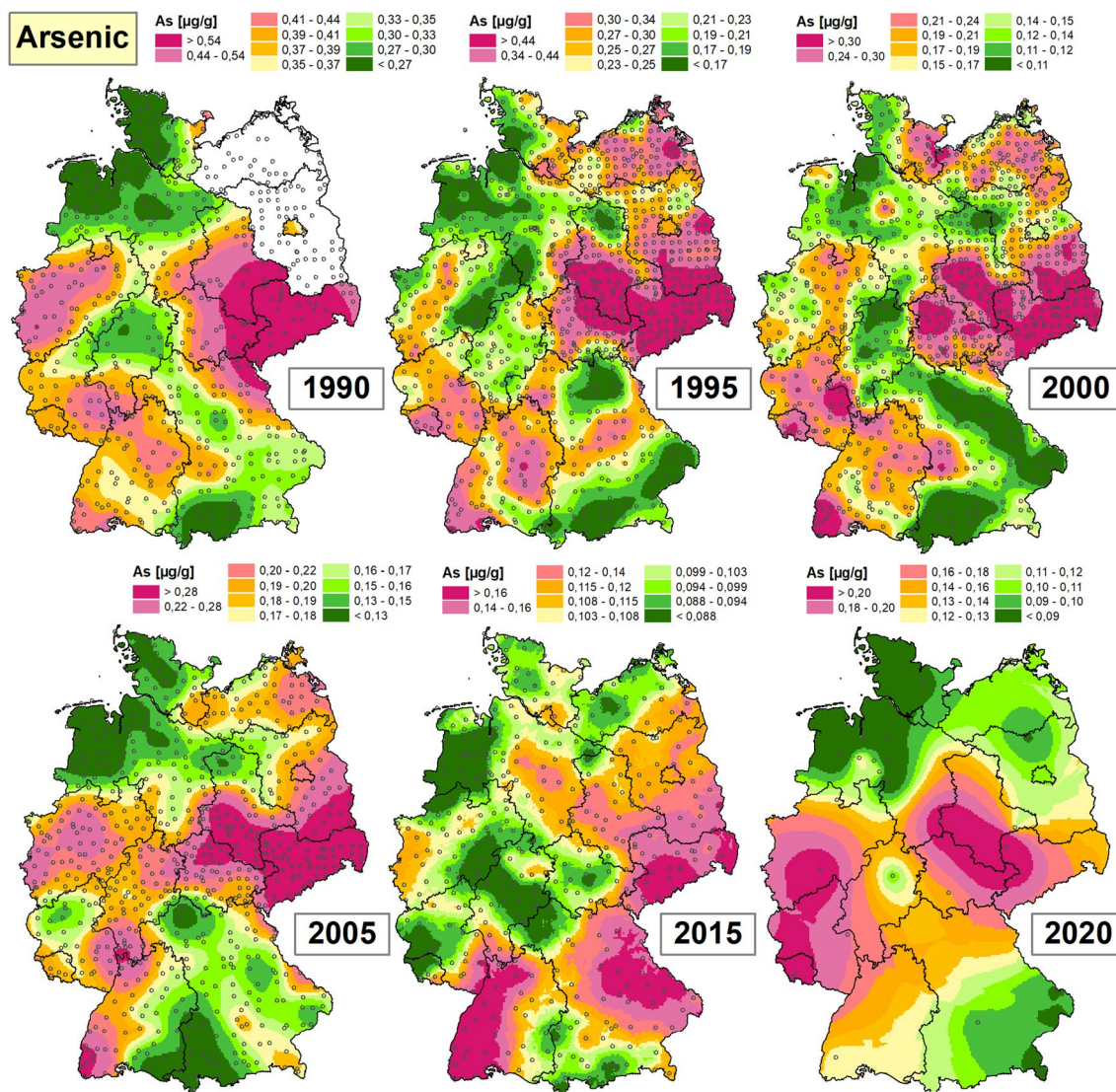


Fig. 4 Geostatistical time series of As concentrations (1990–2020) in mosses (campaign-specific percentile classes)

The geostatistical area estimation of the As concentrations in the mosses was carried out using Ordinary Kriging and was based on the given distribution with log-transformed measured data (Table 7). The exponential model variogram fitted to the experimental semivariogram shows a very strong but non-significant spatial autocorrelation within a range of 305 km (nugget/sill ratio=0; Morans I with $p=0.14$). The cross-validation ratios indicate a relatively unbiased estimate (MSE=− 0.04; RMSSE=1.15) with moderately strong correlations ($r_p=0.43$) and on average low deviations between the measured values and the cross-validation estimates (MPEc=8%) (Table 8).

Table 8 contains key figures estimated using the model functions described in Table 7, which were derived from the respective experimental variograms (Additional file 1: Figures S1–S6). The estimated nugget values are zero in three cases and close to zero in another three. Furthermore, for these findings, as for all other methods of spatially discrete sampling, statements about the characteristics of measured variables at spatial distances below the smallest measuring point distance remain unknown.

The spatial pattern illustrated by the corresponding estimation map results in elevated As area estimates for the year 2020 in Saarland, western Rhineland-Palatinate and southern Saxony-Anhalt as well as in the Leipzig area (Fig. 2; Additional file 1: Figure S1). The maps of the

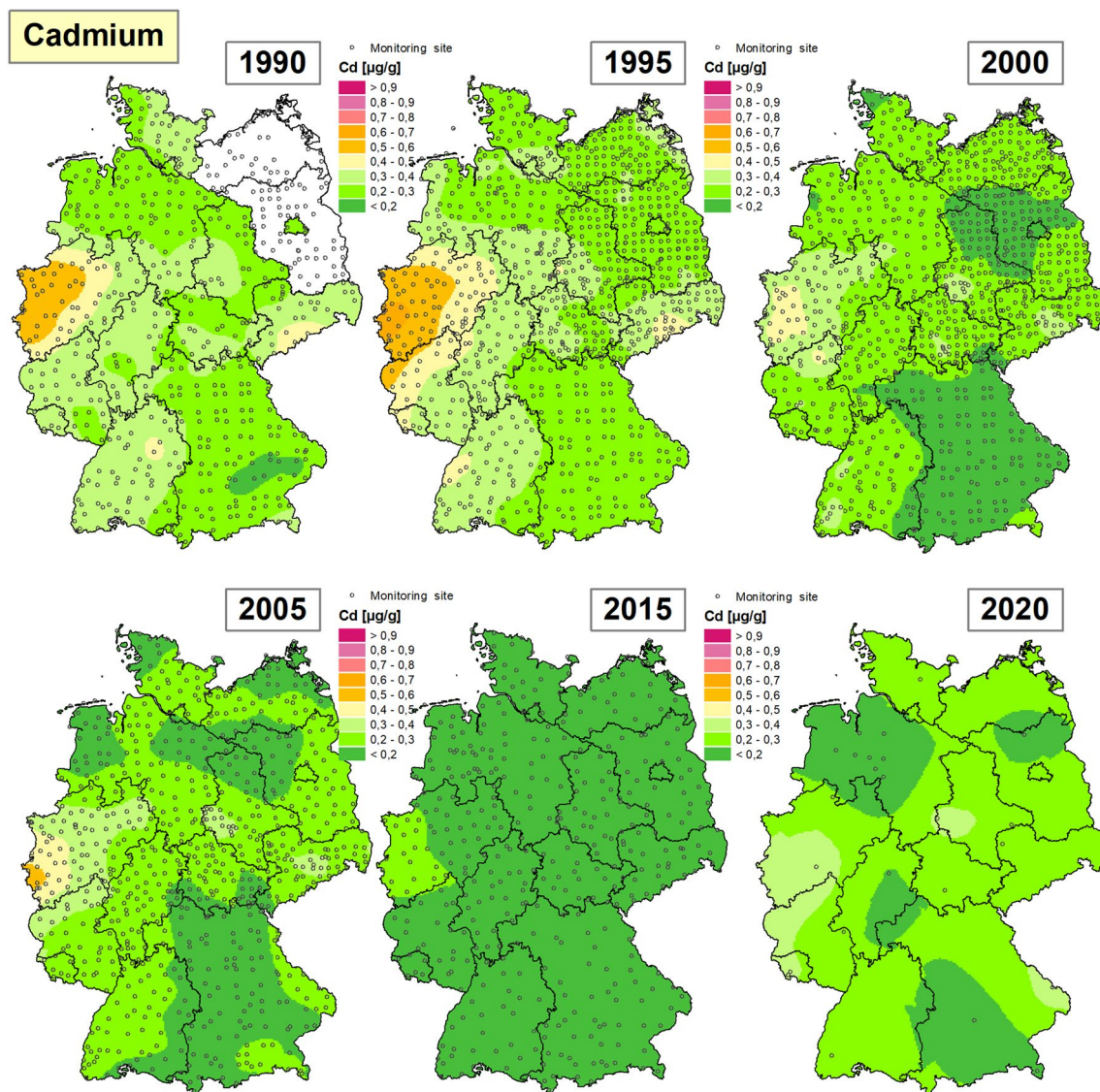


Fig. 5 Geostatistical time series of Cd concentrations in mosses 1990–2020 (measured value classification according to ICP Vegetation [2])

cross-campaign and campaign-specific percentile classes reveal large parts of northern Germany and southern Bavaria as areas with below-average As concentrations in mosses in 2020 (Figs. 3 and 4).

The spatio-temporal development of the nationwide area estimates of As concentrations in the moss is shown in Fig. 3 using the kriging maps calculated for all six campaigns and presented according to cross-campaign percentile statistics. These illustrate an almost continuous nationwide decrease in As bioaccumulations from 1990 to 2000. No significant changes are initially discernible between 2000 and 2005, but further decreases can be observed on a large scale in the period from 2005 to 2015. From 2015 to 2020, the As concentrations in

mosses increased again, especially in Saarland, Rhineland-Palatinate and southern Saxony-Anhalt as well as in the Halle/Leipzig area, but overall they remain below the 2005 level. In the time series presentation of the campaign-specific percentile classes from 1990 to 2020 (Fig. 4), especially Saxony and southern Saxony-Anhalt appear as a consistent hot spot for the bioaccumulation of As in mosses. The area of the northern Upper Rhine can be identified as another consistent hot spot, albeit in a weakened form.

Cd—cadmium The surveys at the 26 MM2020 sites in Germany yielded Cd concentrations in mosses between 0.073 and 0.384 µg/g (Table 2), with the measured values meeting the target value of the M2 standard (Table 1).

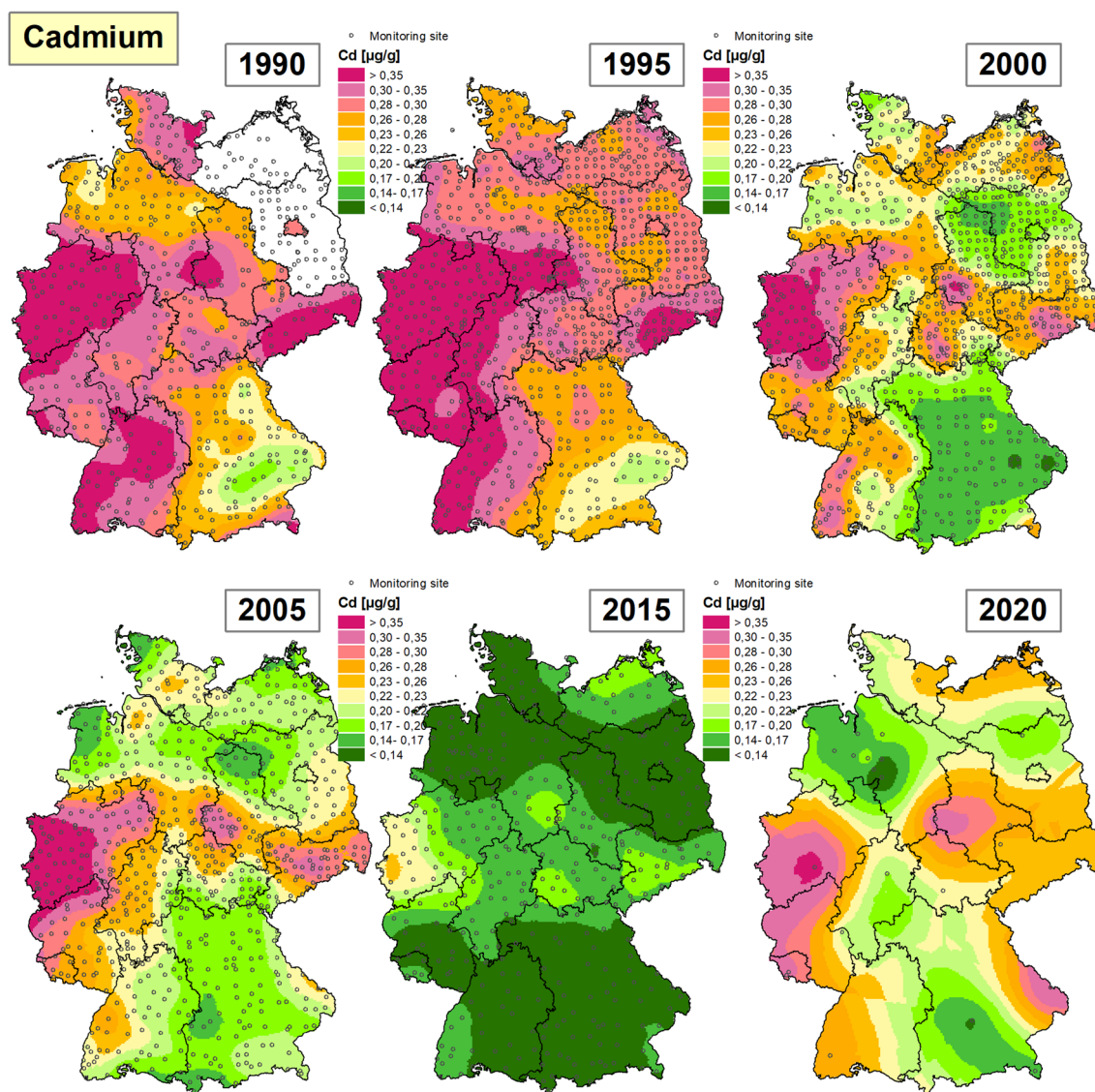


Fig. 6 Geostatistical time series of Cd concentrations in mosses 1990–2020 (cross-campaign percentile classes)

The highest Cd value was measured in a *hypcup sample* in North Rhine-Westphalia east of Cologne (NW27) (Table 3). The median value of 0.210 µg/g (Table 5) is clearly above that of the previous campaign in 2015 (Fig. 1). The sites with Cd levels above the median value are distributed across all federal states.

Since the first sampling in 1990, the Cd concentrations in the mosses have decreased significantly by – 27% until today. After the nationwide increase of the Cd median from 1990 to 1995 by + 2%, there was a decrease of – 28% in 2000, no change between 2000 and 2005, a decrease of – 35% between 2005 and 2015 and a significant increase of + 55% again in 2020 (Tables 5, 6). Thus, the Cd median

of the current campaign is at the same level as in 2000 and 2005.

The spatial generalization of the Cd concentrations in the mosses was carried out using Ordinary Kriging (Table 7). The spherical model variogram fitted to the experimental variogram shows a strong, although not significant, spatial autocorrelation (Moran's I with $p=0.32$) with a range of 228 km and a nugget/sill ratio of 0.11 (Additional file 1: Figure S2). The results of cross-validation indicate a relatively unbiased estimate (MSE = – 0.05; RMSSE = 1.12) with low correlated measured and estimated values ($r_p=0.26$). The average relative deviation, adjusted for SR, between the empirical measured values and the estimated

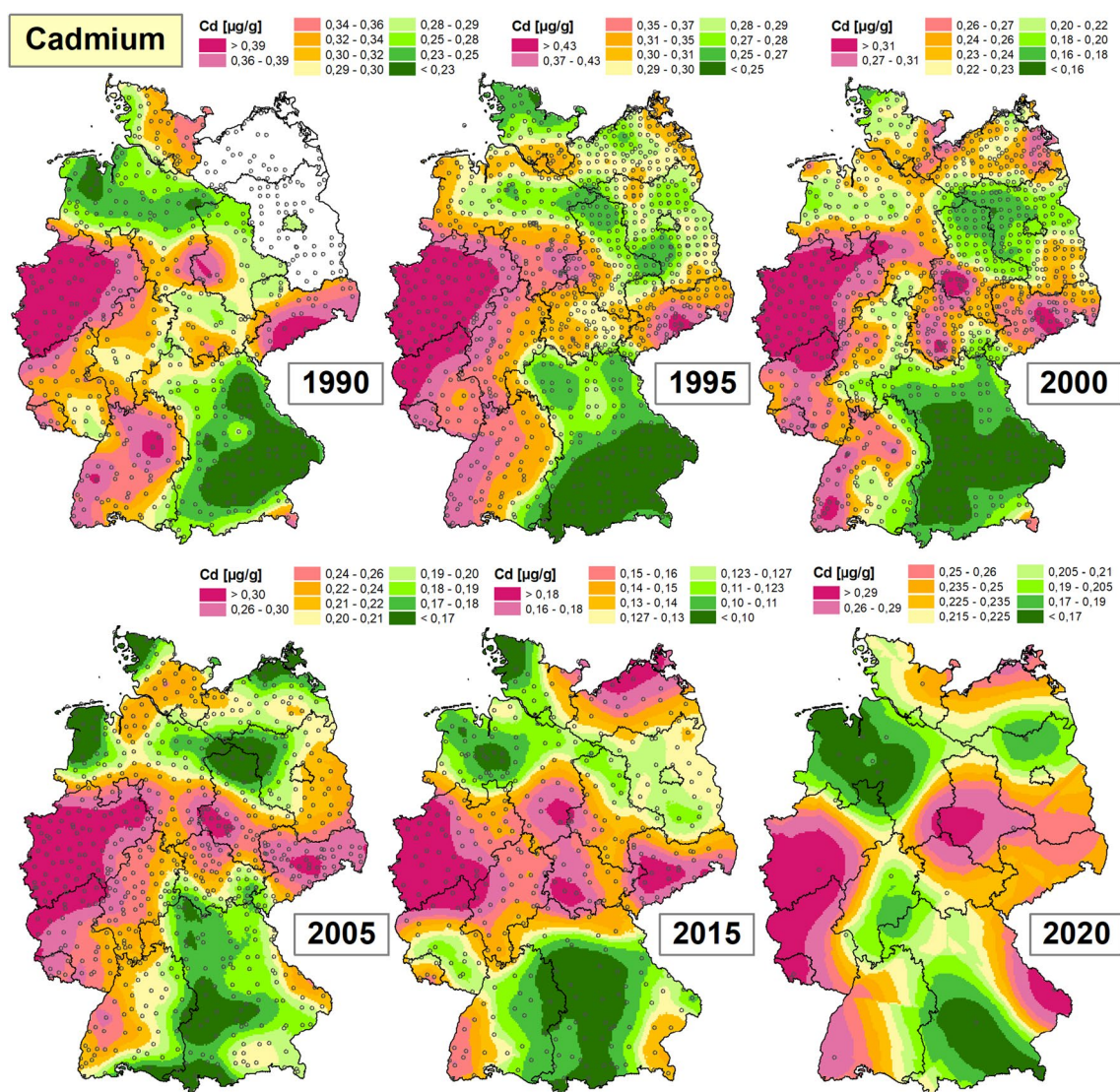


Fig. 7 geostatistical time series of Cd concentrations in mosses 1990–2020 (campaign-specific percentile classes)

values determined via cross-validation (MPEC) is only 1.38% (Table 8). Figure 5 illustrates the spatio-temporal development of Cd bioaccumulation on the basis of the six kriging maps since 1990. After a corresponding increase can initially be observed in the period 1990–1995, the values decrease across the board until 2000. In the period 2000 to 2005, a further decline in Cd bioaccumulation can be seen in northern Germany as well as in Thuringia and Baden-Württemberg. The same can be seen in North Rhine-Westphalia, but there is a small-scale increase in the west of the country. Slight increases can also be seen in Bavaria and Brandenburg. Between 2005 and 2015, Cd levels in moss initially decrease significantly overall, but in the

2020 campaign they return to the 2005 level (Fig. 6). In 2020, increased Cd levels are found in the western parts of North Rhine-Westphalia and Rhineland-Palatinate as well as in Saarland and the Harz Mountains. The spatio-temporal analysis based on the campaign-specific percentile classes from 1990 to the present reveals a consistently broad band of relatively high Cd bioaccumulation from the Lower Rhine to Saxony (Fig. 7).

Cu—copper In MM2020, Cu concentrations between 3.93 and 14.50 µg/g were measured in the mosses at all of the 26 sites visited in Germany (Tables 2, 3). The measurements met the target value of the moss standards M2 and M3 (Table 1). The highest Cu content by far was found in Lower Saxony (NI117_124). Other sites with Cu

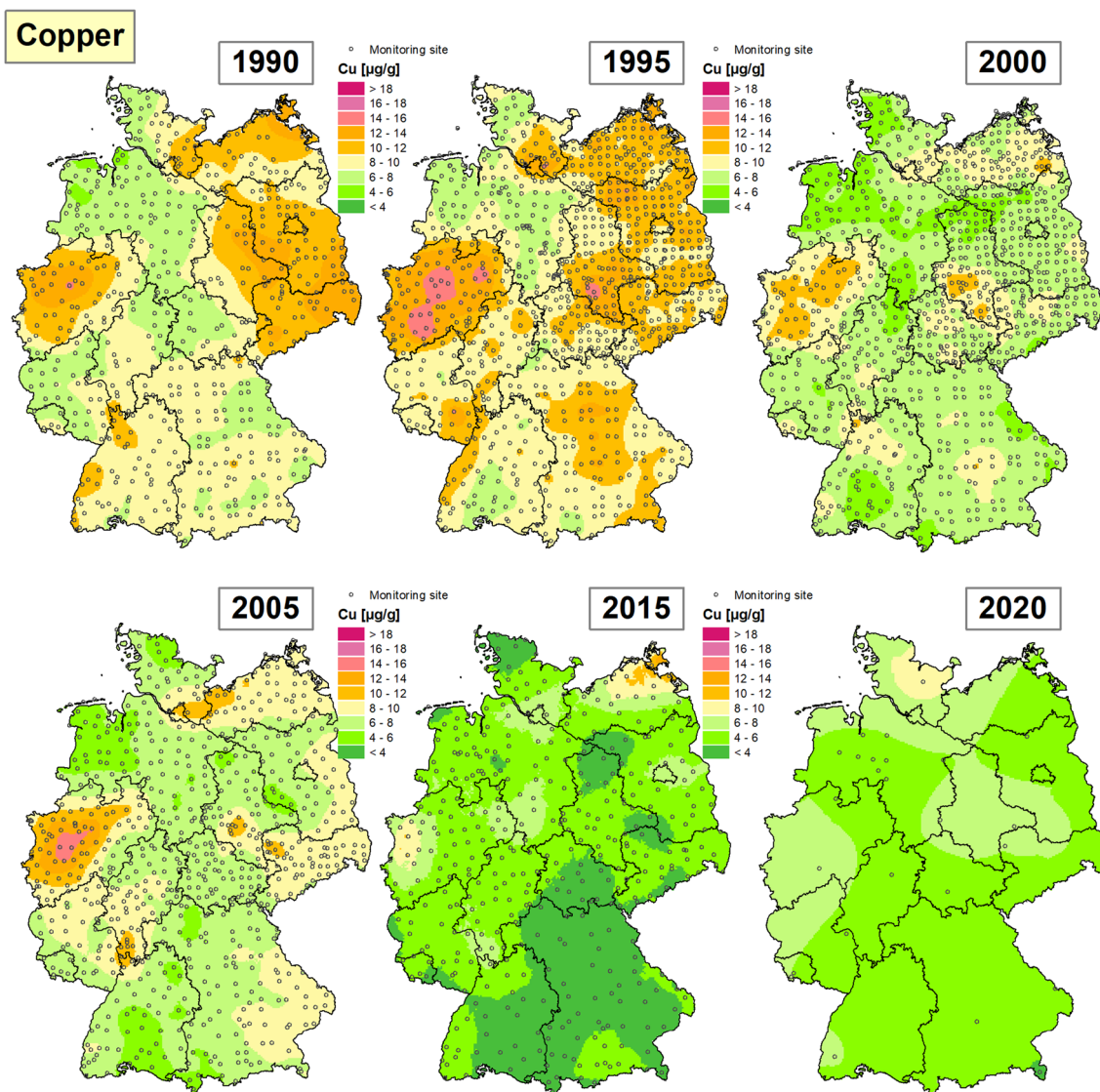


Fig. 8 Geostatistical time series of Cu concentrations in mosses 1990–2020 (measured value classification according to ICP Vegetation [2])

accumulations above the 90th percentile ($7.77 \mu\text{g/g}$) are also found in Lower Saxony and Schleswig–Holstein. The lowest Cu levels below the nationwide 20th percentile of $4.85 \mu\text{g/g}$ were also measured in Lower Saxony as well as in Bavaria and Brandenburg.

Compared to the base year 1990, a declining long-term trend with a decrease of Cu accumulation in the mosses by -33% can be observed. From 1990 to 1995 there are initially no significant changes, between 1995 and 2000 the Cu median decreases by -24% and for the period 2000–2005 there is again no change. Between 2005 and 2015, however, the Cu median decreases again by -36% . Although the current measured values of MM2020 show an unusually significant increase in Cu concentrations

of $+26\%$ since 2015, compared to the previous campaign in 2005, the Cu concentrations in the mosses have decreased by -19% (Tables 5, 6).

The geostatistical area estimation of the measured Cu values was carried out by means of Ordinary-Kriging (Table 7), whereby the spherical model variogram fitted to the experimental variogram indicates a very strong spatial autocorrelation of the measured data (range = 271 km; Nugget/Sill ratio = 0). However, the Morans I statistic does not confirm the significance of the spatial autocorrelation ($p = 0.91$). Cross-validation ratios indicate an unbiased estimate (MSE = -0.03 ; RMSSE = 1.12) and the average relative SR-adjusted deviation between measured and estimated values is low at

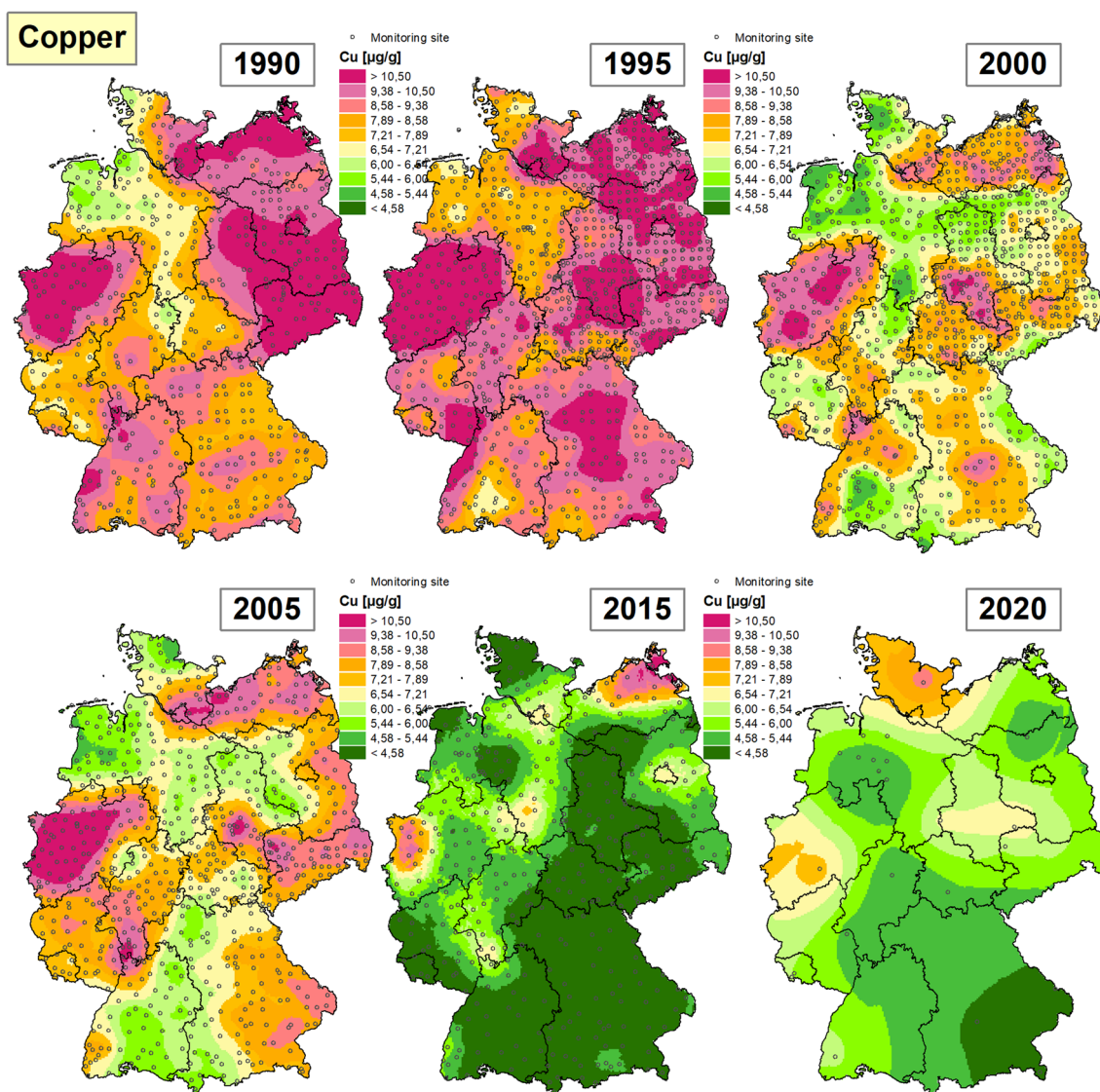


Fig. 9 Geostatistical time series of Cu concentrations in mosses 1990–2020 (cross-campaign percentile classes)

MPEc=5.35% (Table 8). The area map shows medium–high Cu estimates in Schleswig–Holstein and even slightly higher values in the Lower Rhine, Mecklenburg–Western Pomerania, around Hamburg and in Saxony–Anhalt. Low estimates <4.0 µg/g are mainly found in southern Bavaria in the Alpine region (Additional file 1: Figure S3).

The comparison of the kriging maps of all six moss monitoring campaigns (Fig. 8) shows increases in Cu estimates in large parts of south-west Germany for the period from 1990 to 1995. Although decreases can be observed in the new Länder, Cu values in 1995 remain at a similarly high level as in 1990. By the 2000 campaign, Cu bioaccumulation is clearly decreasing across the

board, so that areas with increased Cu values can only be found in eastern Mecklenburg–Western Pomerania, southern Saxony–Anhalt and North Rhine–Westphalia (Ruhr area). From 2000 to 2005, increases in Cu content estimates can be observed throughout the eastern part of the Federal Republic, in the Hamburg–Lübeck area, as well as in Hesse, Rhineland–Palatinate and North Rhine–Westphalia. Between 2005 and 2015, estimates of Cu concentrations decrease significantly in most parts of Germany. Increases are only recorded in parts of Mecklenburg–Western Pomerania during this period. From 2015 to 2020, the Cu content in mosses increases in most regions of Germany, but remains below the 2005 level, with the exception of Schleswig–Holstein. Looking at

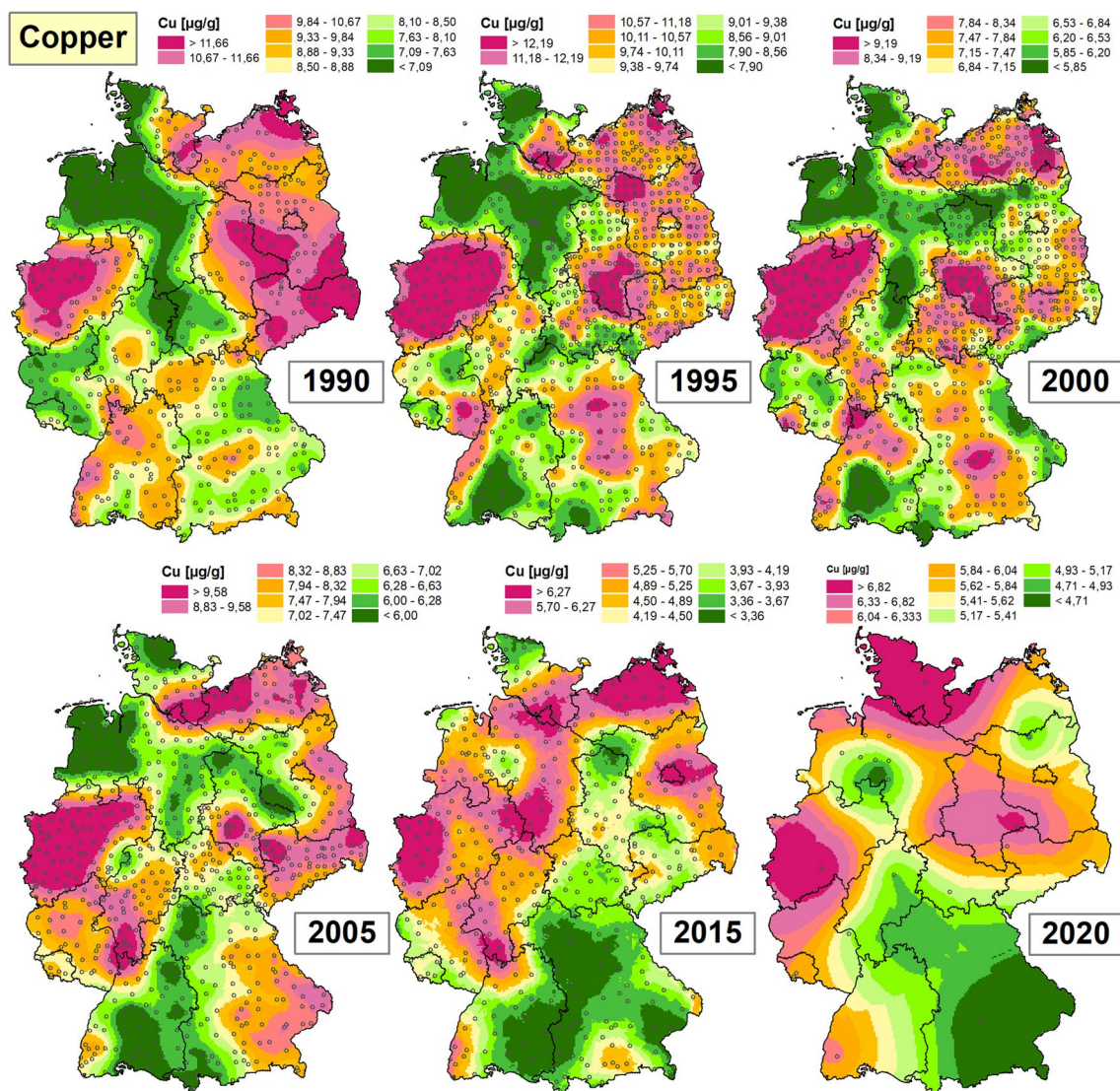


Fig. 10 Geostatistical time series of Cu concentrations in mosses 1990–2020 (campaign-specific percentile classes)

the spatial distribution of the percentiles of the area estimates over time (Figs. 9 and 10), from 1990 to 2020 parts of Mecklenburg–Western Pomerania and Schleswig–Holstein, North Rhine–Westphalia and Hamburg in particular are consistently hot spots of increased Cu enrichment in mosses.

Ni—nickel The Ni concentrations measured in the moss samples during the 2020 campaign ($n=26$, Table 2) provide a median value of 1.800 µg/g and vary between 0.640 and 5.016 µg/g (Table 3). The highest Ni value was determined in a *hypcup* sample near Leipzig (SN240_1). Sites with Ni levels above the 90th percentile (3.811 µg/g) occur in North Rhine–Westphalia and in Hesse. Low Ni concentrations below the 20th percentile (1.256 µg/g)

are found in Lower Saxony and Brandenburg. The target values of the M2 and M3 reference standards are met (Table 1).

The development of the median values of all six campaigns in Germany over time gives the following picture: In the period 2000–2005, after always significant decreases, there is for the first time an—albeit non-significant—increase in the element medians at the federal level (+2.7%). From 2005 to 2015, a significant decrease of – 41.3% can be observed again. From 2015 to the current 2020 campaign, on the other hand, an exceptionally high increase of +165% can be observed. In Germany, however, there has been a significant decrease of – 23% in the Ni median since 1990 (Table 5).

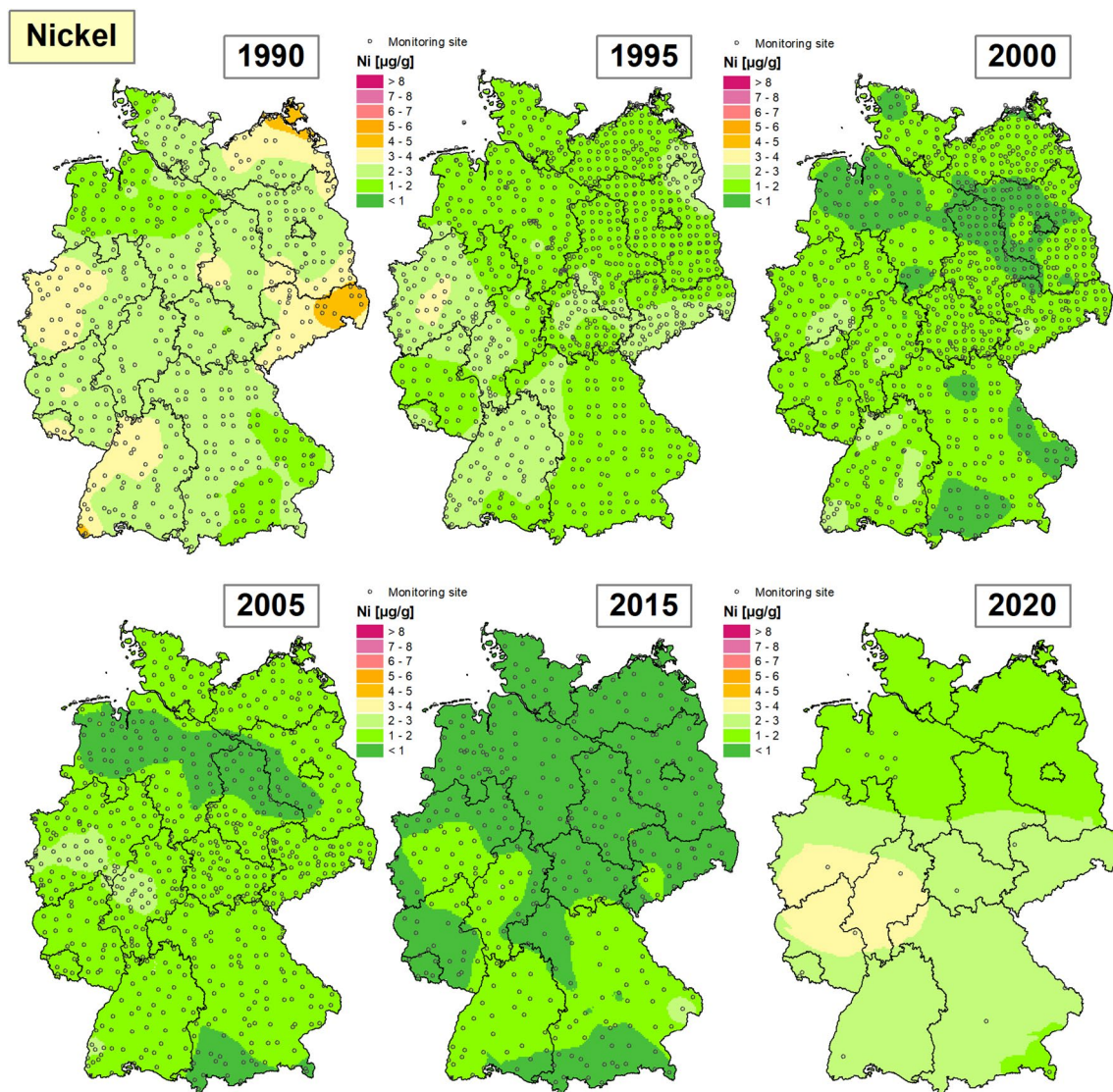


Fig. 11 Geostatistical time series of Ni concentrations in mosses 1990–2020 (measured value classification according to ICP Vegetation [2])

The nationwide area estimation of the Ni concentrations for the year 2020 was carried out by means of ordinary kriging of the previously log-transformed measured values (Table 7). The spherical model variogram fitted to the experimental variogram using the method of least squares shows a moderately strong and weakly significant spatial autocorrelation (Moran's I with $p < 0.1$) in a range of 386 km and a nugget/sill ratio of 0.42 (Additional file 1: Figure S4). The cross-validation ratios indicate that the spatial correlation between the experimental and the experimental variograms is significant. The cross-validation ratios indicate a low biased estimate ($MSE = 0.03$; $RMSSE = 0.91$) with a medium strong correlation between measured and estimated values ($r_p = 0.51$).

The relative cross-validation errors adjusted are on average $MPEc = 20.56\%$ (Table 8). As Fig. 11 shows, the map of the geostatistical area estimates for the year 2020 calculated from the measured values shows areas with elevated Ni concentrations in moss in large parts of North Rhine-Westphalia, Hesse and Baden-Württemberg.

The spatio-temporal development of Ni bioaccumulation in Germany is shown in Fig. 11 on the basis of the kriging maps of the six moss monitoring campaigns carried out so far. These show an area-wide decline in Ni bioaccumulation in the period from 1990 to 1995. The subsequent period between 1995 and 2000 is characterized by a further decrease in nationwide Ni bioaccumulations. From 2000 to 2005, the area

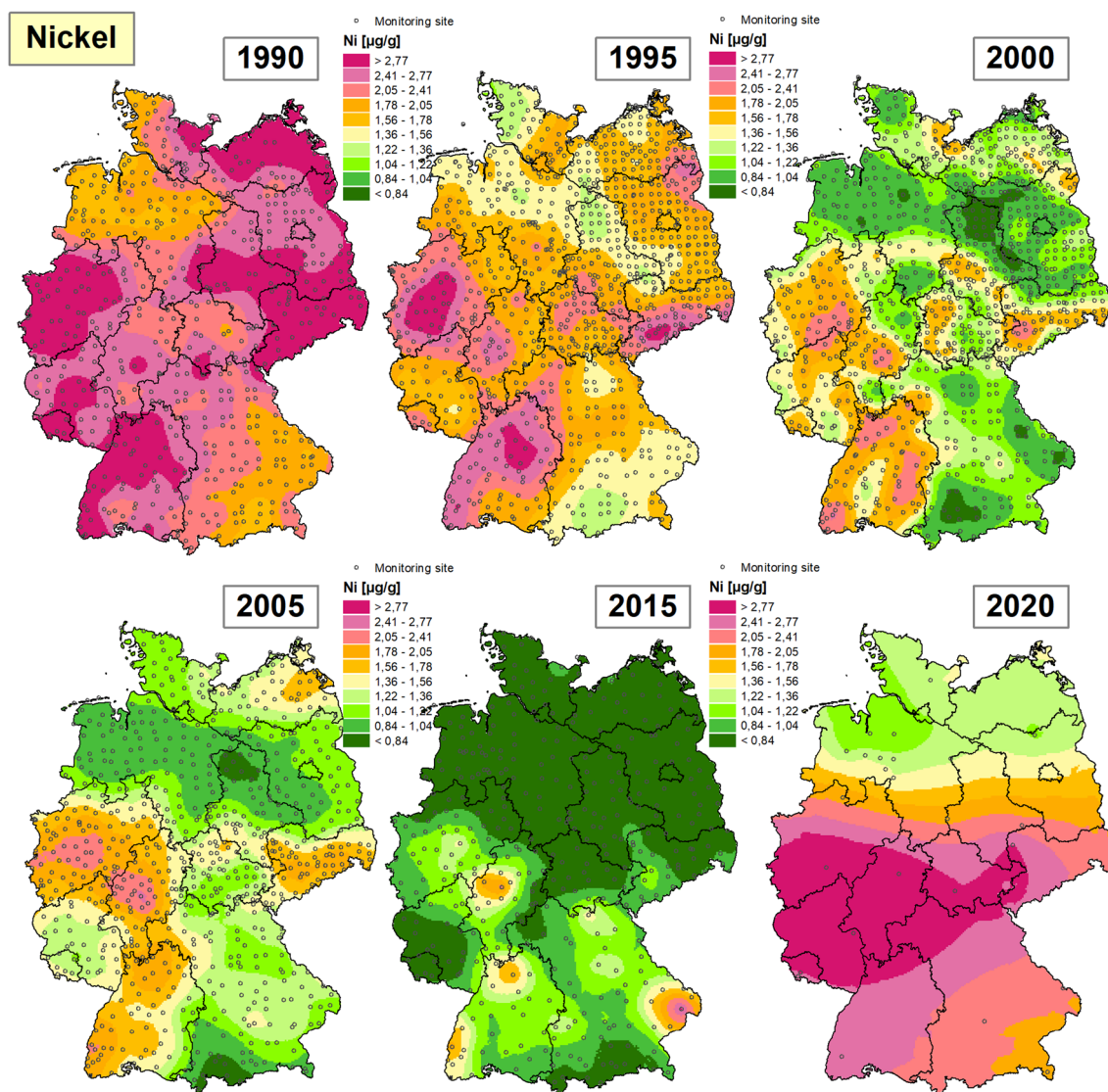


Fig. 12 Geostatistical time series of Ni concentrations in mosses 1990–2020 (cross-campaign percentile classes)

estimates show slight increases in Ni levels in the north of Schleswig–Holstein, in North Rhine–Westphalia (Ruhr area) and Hesse, as well as in Brandenburg and Bavaria. For the period 2005 to 2015, increases can only be observed in parts of Bavaria, whereas in the remaining parts of Germany there are area-wide decreases in the estimated Ni enrichment in the mosses. In the last five years from 2015 to 2020, Ni concentrations in mosses have increased exceptionally strongly in all parts of Germany and are roughly similar to the levels and spatial distributions of the years 1990 and 1995 (Fig. 12). Hot spots with consistently relatively high Ni concentrations in mosses since 1990 are found in North

Rhine–Westphalia, the northern Upper Rhine and in the Leipzig area (Fig. 13).

Pb—lead For lead, the M2 target value is slightly underestimated, M3 is in the target range (Table 1). In MM2020, Pb levels of 0.61 to 11.18 $\mu\text{g/g}$ with a median of 1.88 $\mu\text{g/g}$ were determined at 26 sites in Germany. The highest value nationwide was measured in a *Hypcup sample* in Saarland (SL9_2) (Tables 2, 3). Further elevated Pb concentrations above the 90th percentile (6.73 $\mu\text{g/g}$) are found in moss samples from North Rhine–Westphalia and Saxony–Anhalt. The sites with the lowest values are in Lower Saxony, Brandenburg and Bavaria.

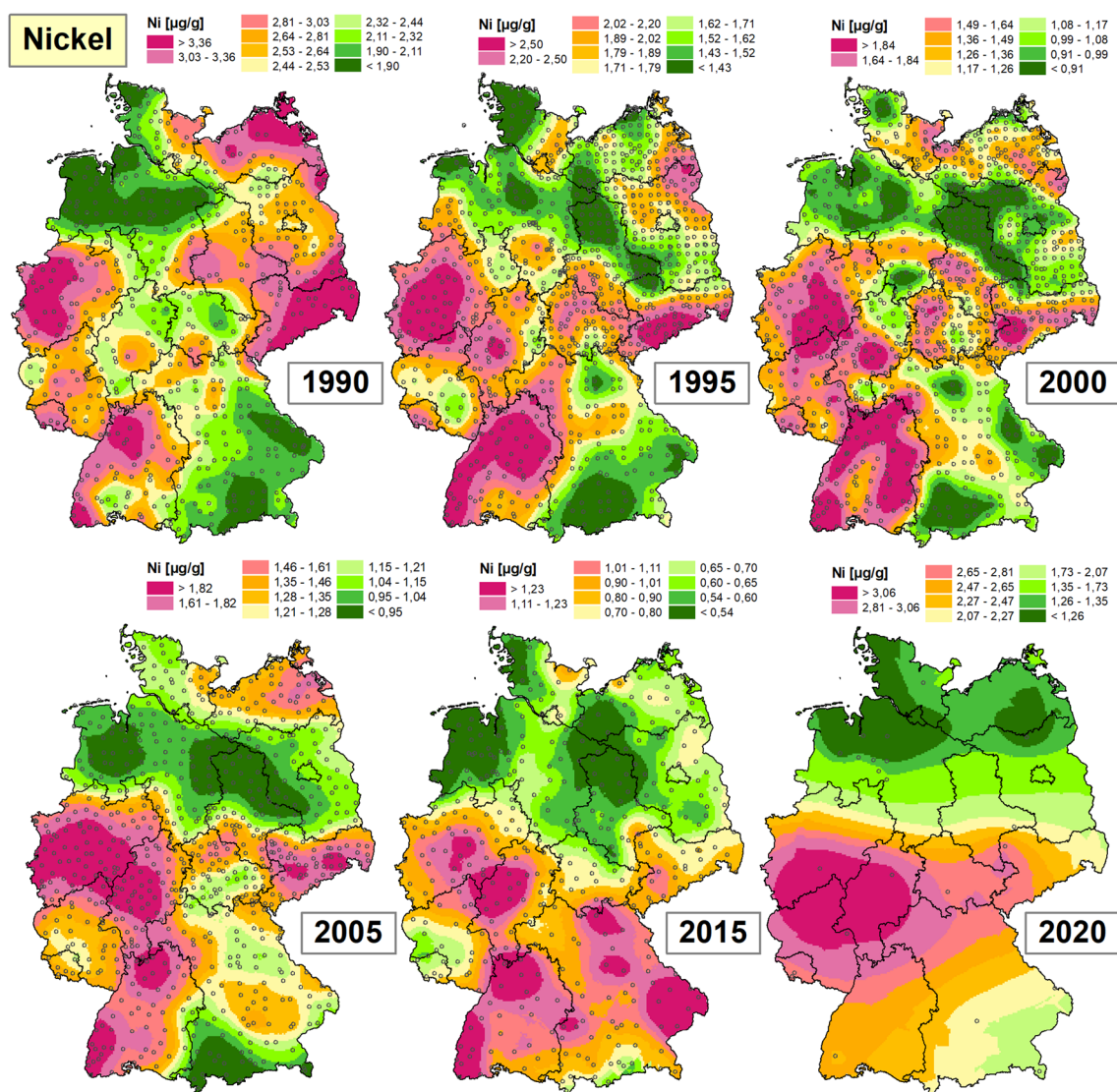


Fig. 13 Geostatistical time series of Ni concentrations in mosses 1990–2020 (campaign-specific percentile classes)

The accumulation trend shows very significant decreases in the nationwide Pb medians between all monitoring campaigns up to 2015. However, the current readings from MM2020 show no significant changes compared to the previous campaign in 2015. The long-term trend 1990–2020 continues to be characterized by a significant decrease of -86% at the federal level (Tables 5, 6) (Fig. 13).

The areal determination of the Pb bioaccumulation in MM2020 was carried out using ordinary kriging based on the previously log-transformed measured values (Table 7). The spherical model variogram shows a strong but non-significant spatial autocorrelation (Moran's I with $p=0.24$) with a range of 137 km and a nugget/

sill ratio of 0.28 (Additional file 1: Figure S5). The Mean Standard Error (MSE) of -0.05 obtained by cross-validation indicates a relatively unbiased estimate, the RMSSE is 0.85. Furthermore, a weak correlation between the measured and estimated values ($r_p=0.38$) was calculated for the model with an average percentage corrected error of $MPEc=25.7\%$ (Table 8). The map of the 2020 geostatistical area estimate shows predominantly areas with low Pb concentrations $< 5 \mu\text{g/g}$ (Fig. 14). Areas with slightly elevated values of Pb enrichment between 6 and $10 \mu\text{g/g}$ are noticeable in North Rhine-Westphalia, Saarland, western Rhineland-Palatinate and in the area of the Harz Mountains.

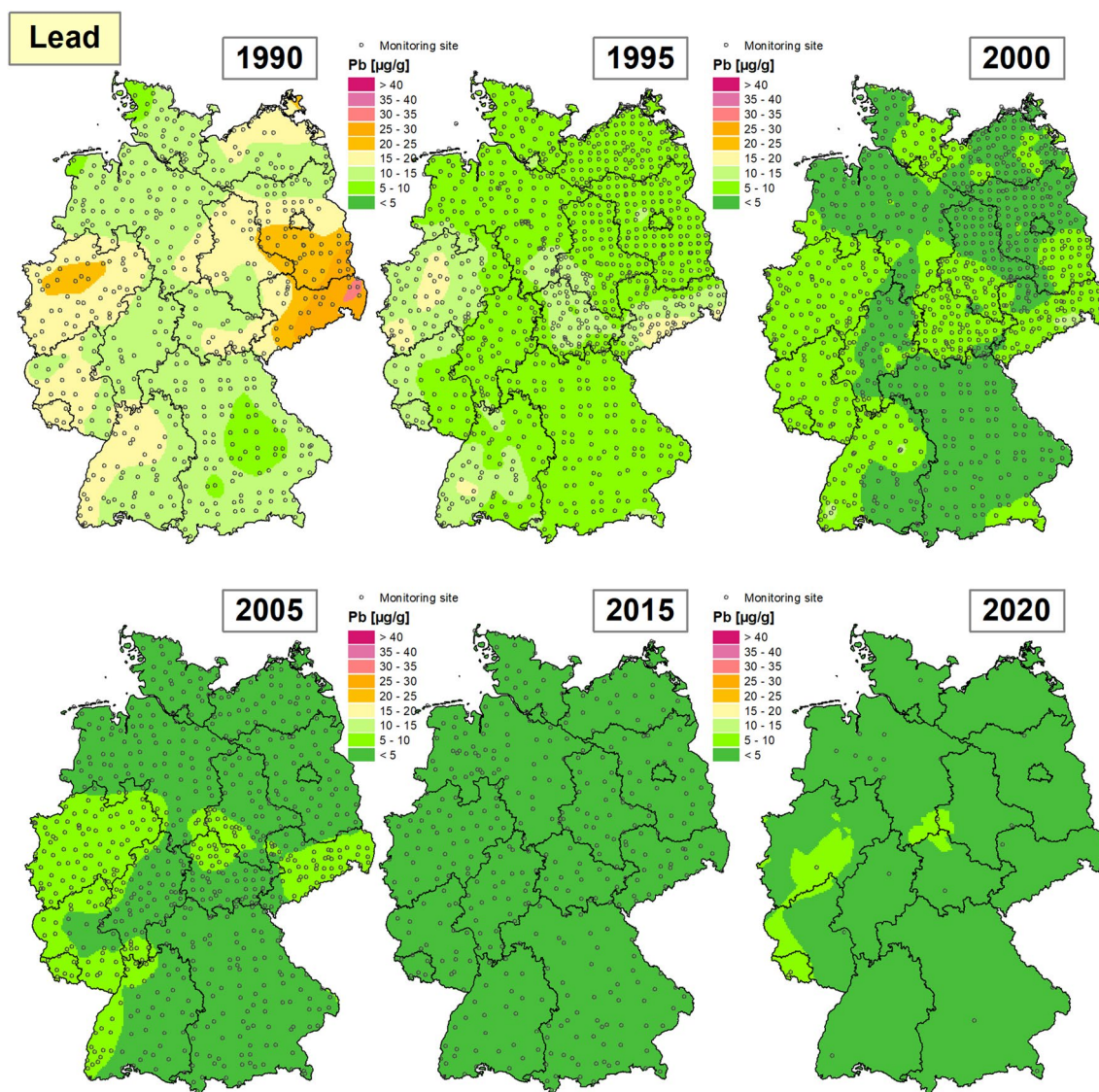


Fig. 14 Geostatistical time series of Pb concentrations in mosses 1990–2020 (measured value classification according to ICP Vegetation [2])

Figure 14 shows the spatio-temporal trend of Pb bioaccumulation based on the kriging maps of the measurement campaigns from 1990 to 2020. These show an area-wide decline in Pb values for the subperiods from 1990 to 2015, with the strongest declines in North Rhine-Westphalia and in some regions of southern Brandenburg and Saxony (Lausitz and Erzgebirge). However, in the period between the last two measurement campaigns in 2015 and 2020, contrary to this long-term trend, a slight increase can be observed again in most regions of Germany—with the exception of Schleswig–Holstein and large parts of Lower Saxony—although the 2005 level is generally not reached (Fig. 15). In the time series of the six campaign-specific

percentile maps (Fig. 16), North Rhine-Westphalia, Saarland, the Harz Mountains as well as the Ore Mountains can be identified as consistent focal areas of Pb enrichment in mosses, while large parts of northern Germany and Bavaria have always had the lowest Pb concentrations since 1990.

Sb—antimony The target values of the M2 and M3 reference standards are met (Table 1). The Sb concentrations in the mosses determined nationwide at the 26 sites give a median value of 3.087 µg/g and lie overall between 0.080 and 0.388 µg/g. The maximum was measured in a *hypcup* sample taken in North Rhine-Westphalia (NW27). The maximum was measured in a *hypcup* sample taken in North Rhine-Westphalia (NW27) (Tables 2,

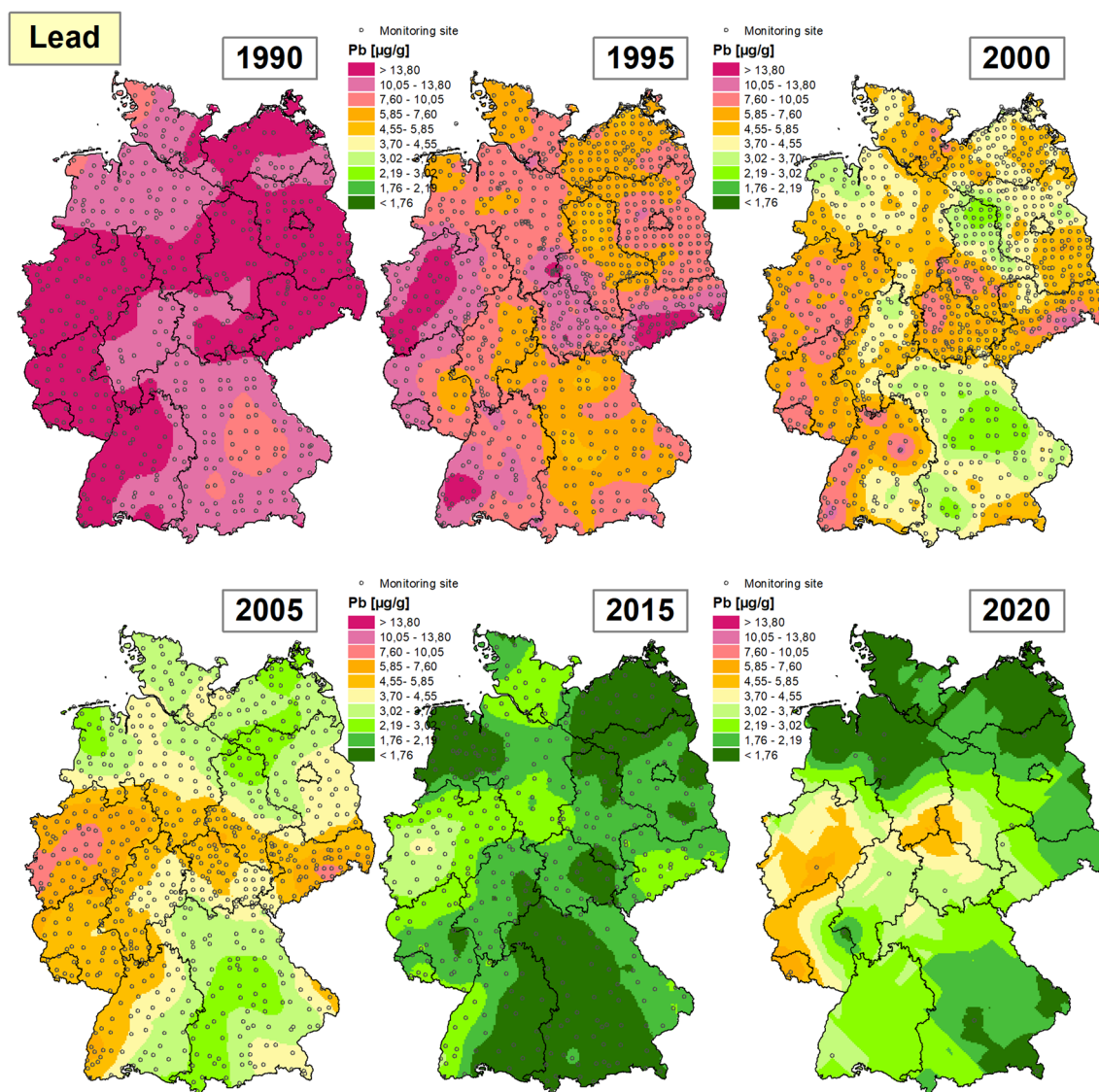


Fig. 15 Geostatistical time series of Pb concentrations in mosses 1990–2020 (cross-campaign percentile classes)

3). The spatial distribution shows Sb levels above the 90th percentile ($0.217 \mu\text{g/g}$) predominantly in North Rhine-Westphalia and in Saxony-Anhalt. Low Sb concentrations below the 20th percentile ($0.122 \mu\text{g/g}$) are found nationwide distributed over Bavaria, Hesse, Lower Saxony, Rhineland-Palatinate and Saarland.

As can be seen in Table 6, after a significant decrease in the nationwide Sb medians in the period from 1995 to 2000 (-13%), a significant increase of 7% can be observed in the period from 2000 to 2005 and a decrease of -44% again between 2005 and 2015. Since the last campaign between 2015 and 2020, an increase of $+64\%$ can be observed again. The long-term trend

from 1995 to 2015 at the federal level continues to show a significant decrease in the Sb medians (-14%).

The spatial generalisation of the Sb values was carried out using ordinary kriging of the previously log-transformed measured values (Table 7). The spherical model variogram fitted to the experimental variogram shows a nugget/sill ratio of 0.25 within the radius of 224 km and thus a strong spatial autocorrelation, which proves to be weakly significant despite the few measurement points (Moran's I with $p=0.08$). However, the measures of cross-validation indicate a slightly biased estimate ($\text{MSE} = -0.1$; $\text{RMSSE} = 1.31$) with an implausible correlation of the measured and estimated values of -0.45 (Additional file 1: Figure S6). However, the average

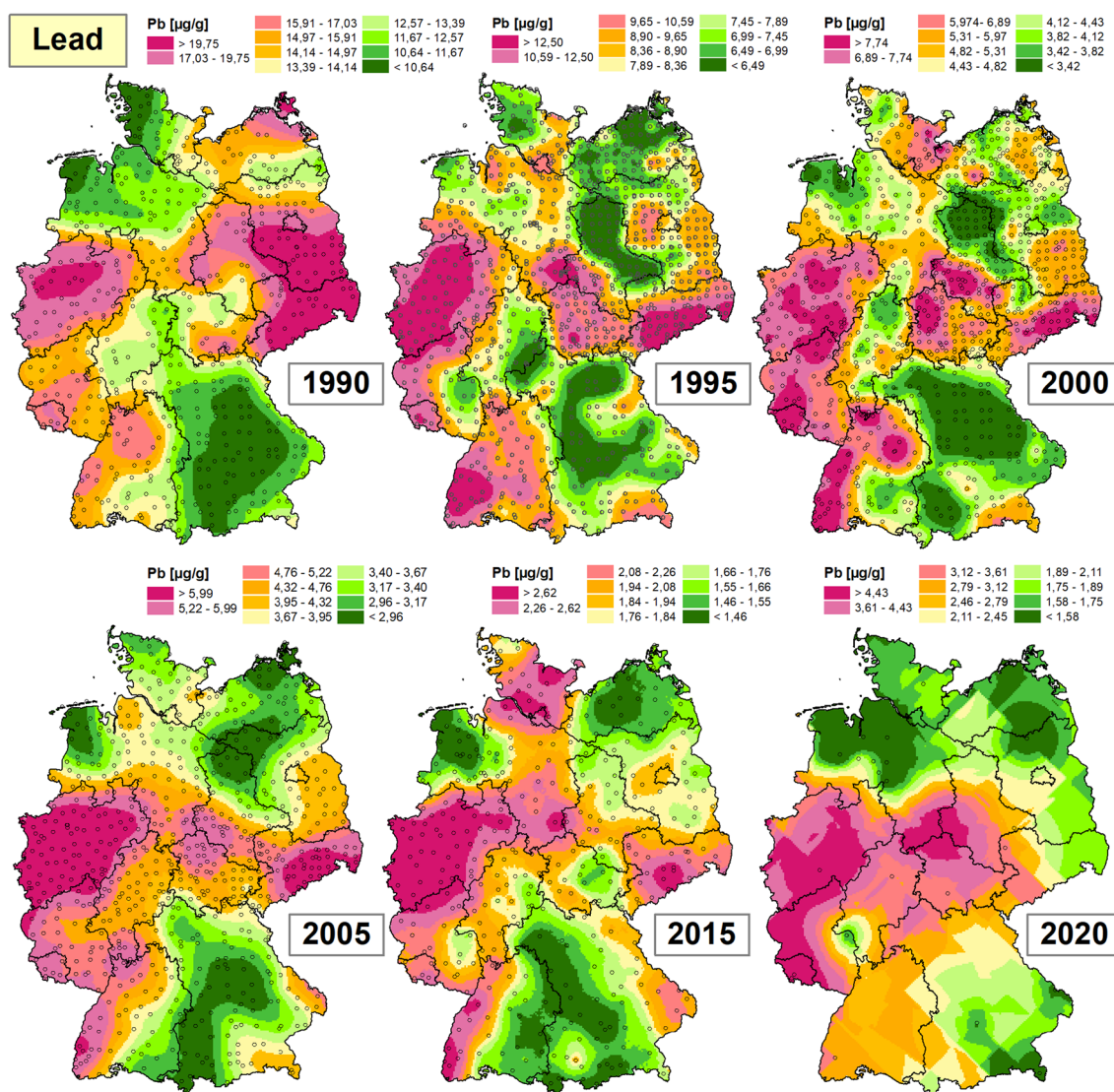


Fig. 16 Geostatistical time series of Pb concentrations in mosses 1990–2020 (campaign-specific percentile classes)

discrepancy between the measured values and cross-validation estimates multiplied by SR remains low and amounts to $MPEc = 4.47\%$ (Table 8). As Fig. 17 shows, the focus of elevated Sb estimates in 2020 is in North Rhine-Westphalia, while the rest of Germany has low Sb concentrations ($< 0.2 \mu\text{g/g}$). According to the current campaign, the lowest Sb values ($< 0.12 \mu\text{g/g}$) are found in Lower Saxony, Hesse and Rhineland-Palatinate.

The spatio-temporal development of Sb bioaccumulation shown in Fig. 17 on the basis of five kriging maps shows area-wide decreases, some of them significant, in the period from 1995 to 2000. In the period from 2000 to 2005, the area estimates in North Rhine-Westphalia (Ruhr area), Hesse, Rhineland-Palatinate, Saxony and

Bavaria show an increase in Sb concentrations again. A decrease in values can be observed especially in Saarland. Between the 2005 and 2015 measurement campaigns, further significant decreases can be observed throughout Germany, but Sb concentrations increase again from 2015 to 2020 in most parts of Germany (Figs. 18, 19), so that the nationwide pattern of Sb levels in 2020 again approximates that of 2005. Consistent focal areas of Sb bioaccumulation emerge in the campaign-specific evaluation since 1995 for North Rhine-Westphalia and the Ore Mountains (Fig. 19).

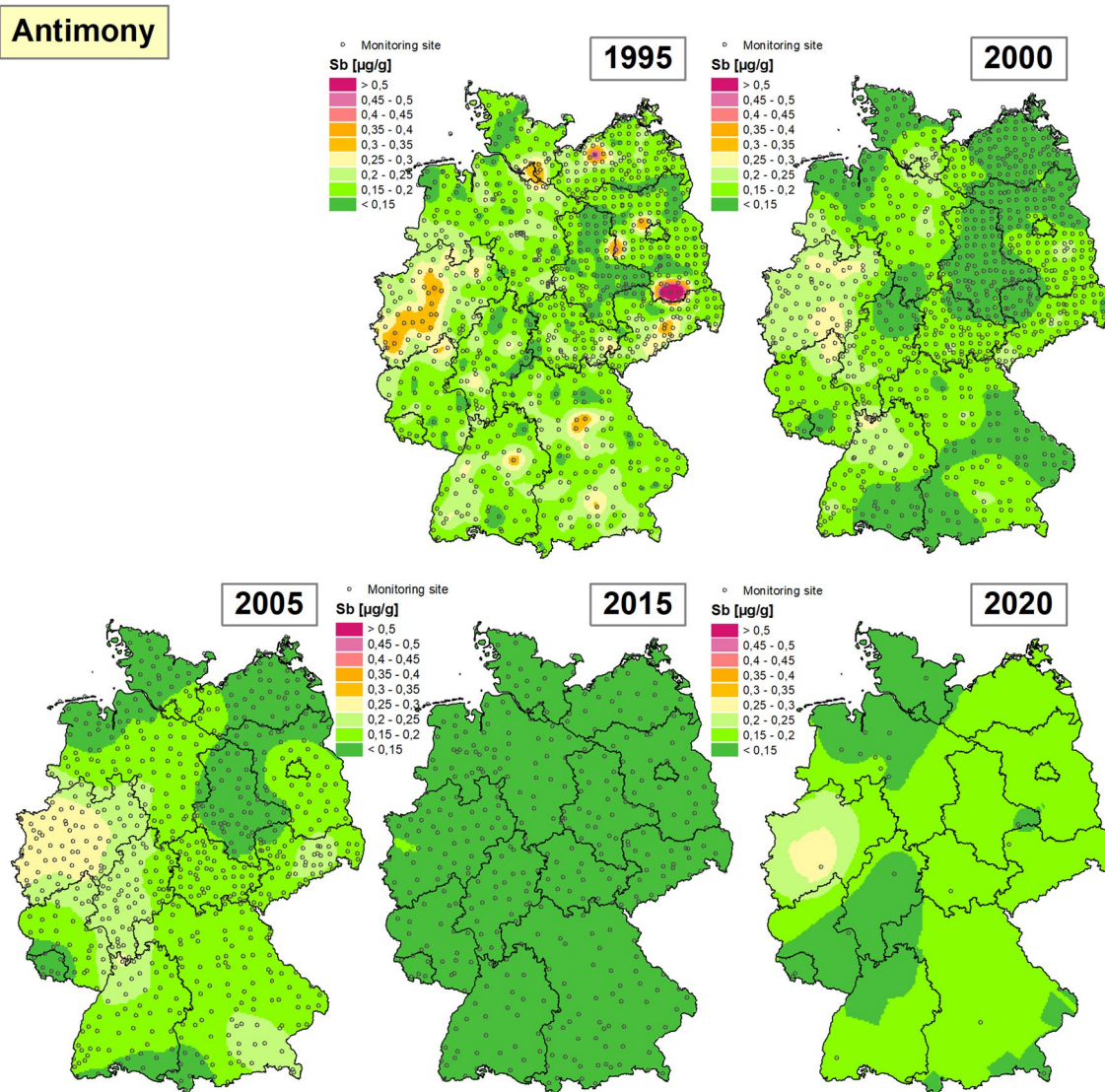


Fig. 17 Geostatistical time series of Sb concentrations $\mu\text{g/g}$ in mosses 1990–2020 (measured value classification according to ICP Vegetation [2])

Discussion

The decreases recorded for all heavy trace elements in the period between MM2005 and MM2015 did not continue in the current campaign. On the contrary, for four of the six trace elements investigated (Cd, Cu, Ni and Sb) higher concentrations were measured in the moss samples in MM2020 than in MM2015 (Table 6). The range extends from +26% (Cu) to +165% (Ni). For As and Pb, on the other hand, no significant changes compared to 2015 can be observed. The long-term trend is different when comparing the current median values with those of the base year (=year of first sampling): Since 1990, the median concentrations of As, Cd, Cu, Ni, Pb and Sb in

the mosses have decreased significantly, with the strongest decrease being recorded for Pb (-86%).

Six of the twelve elements investigated had to be excluded from consideration in advance, as either the measured values of 2015 at the 26 MM2020 sites already differed significantly from those of the total MM2015 sample ($n=397$ to 400) (Al, Cr, Fe, V and Zn) or the moss standards in the quality assurance were overestimated by 50 to 100% (Hg).

In principle, it must be taken into account that the determined temporal trends may be significant in a statistical sense, but it cannot be ruled out that small-scale measurement variability, for example due to crown effects [23], may influence them. Another factor

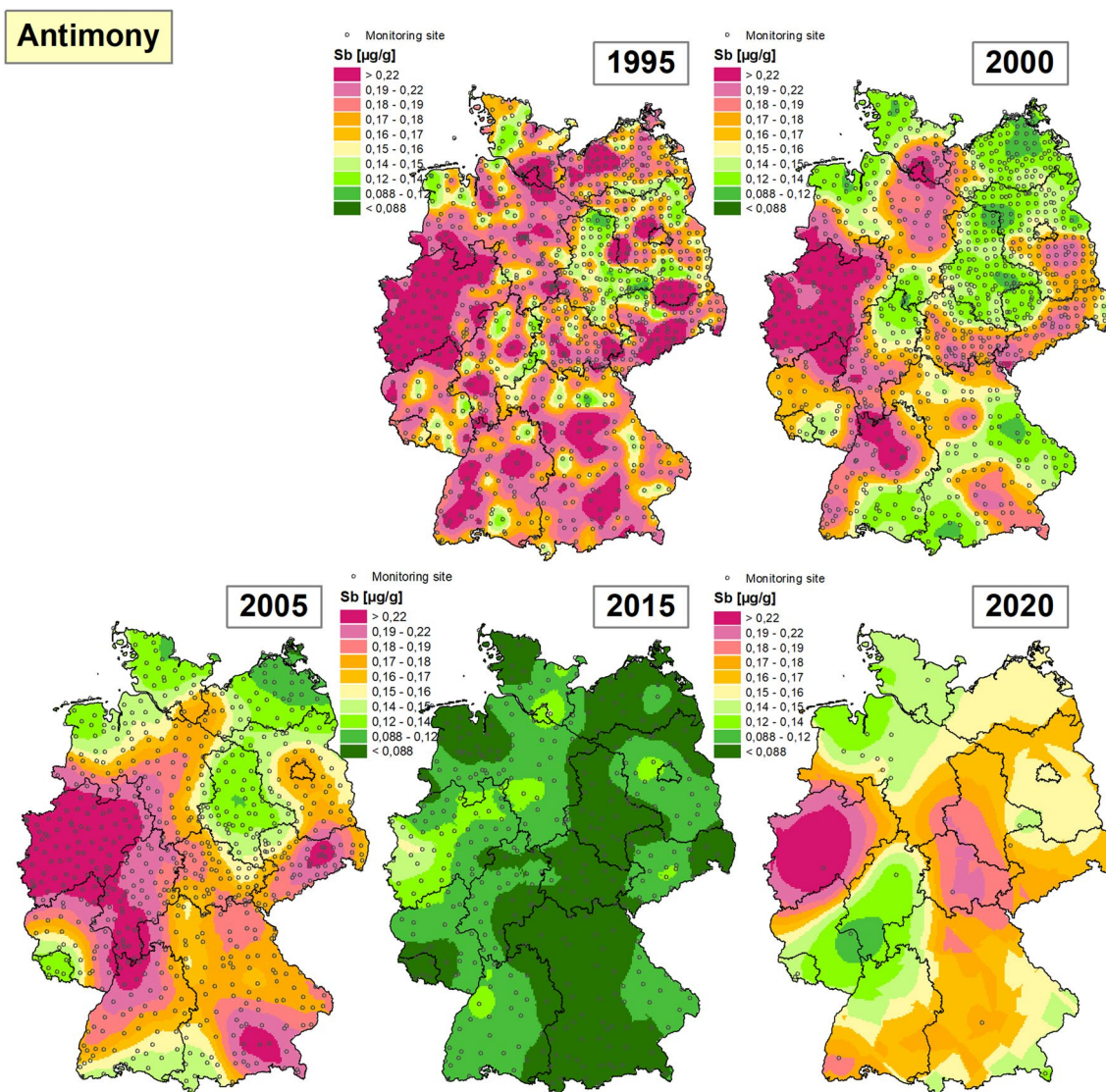


Fig. 18 Geostatistical time series of Sb concentrations in mosses 1990–2020 (cross-campaign percentile classes)

of estimation accuracy for the central tendency is the small number of cases ($n=26$) in the current campaign. The minimum sample numbers (MPZ=number of sites) calculated for the 12 standard elements and nitrogen in MM2015 according to the SSAD (Sample Size for Arbitrary Distributions) method [24, 25] can serve as a benchmark for assessing this issue for compliance with an error tolerance of 20% in the calculation of the arithmetic mean ($\alpha=0.05$). Accordingly, based on the sample sizes evaluated in MM2020, the largest inaccuracies (> 20%) are to be expected for As, Cd, Cu, Ni and Pb. For the remaining trace elements, the minimum sample numbers are also not achieved in the MM2020.

Looking at the confidence intervals that include the true median value of 2022 with a 95% probability, the upper limits of these intervals in 2015 are clearly below the lower limits of the intervals of 2020 for Ni and Sb, and still slightly below the lower limits of the intervals of 2020 for Cd and Cu. This means that the probability that there was an actual increase in these element concentrations between 2015 and 2020 is over 95%.

Furthermore, with regard to the small sample size in 2020, it should be borne in mind that the degrees of freedom are further reduced in the case of spatially autocorrelated data (especially in Lower Saxony) and that this can have an impact on the significance test

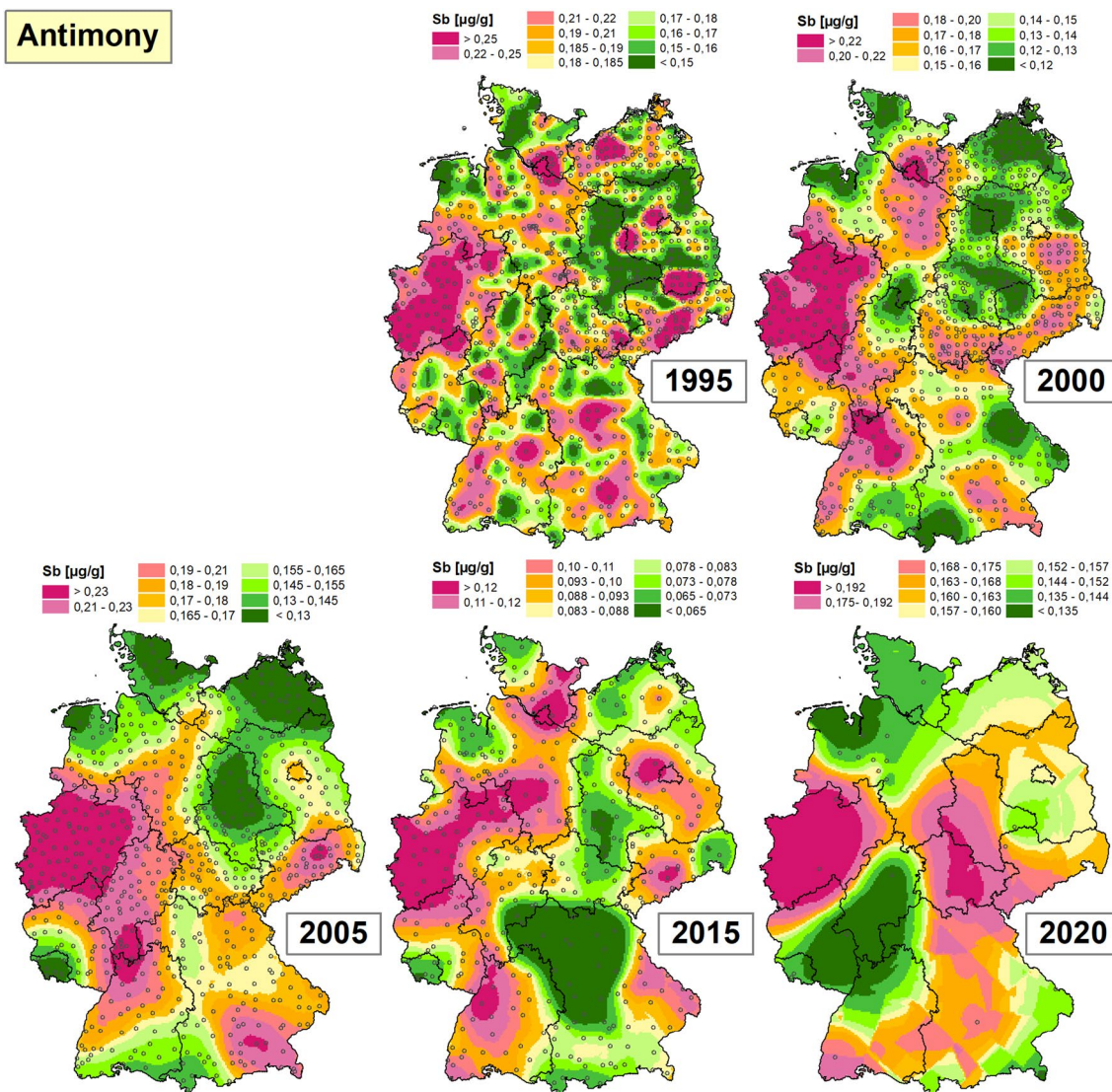


Fig. 19 Geostatistical time series of Sb concentrations in mosses 1990–2020 (campaign-specific percentile classes)

in the inferential statistical trend analysis. In the geostatistical area estimates, the low spatial density of the sampling network also leads to the fact that the spatial autocorrelation is to be classified as non-significant for five of the six trace elements examined in MM2020. Furthermore, compared to the previous campaigns, the spatial autocorrelation ranges are mostly much larger, up to 386 km, within which the spatial interpolation is carried out, which leads to relatively low spatial differentiations of the area estimates.

Furthermore, at the 26 sites of 2020, fourteen samples were collected from completely different moss sampling areas than in MM2015, which are located within the 2 km radius permitted by the Moss Manual, but which

in some cases show deviating deposition conditions (e.g., vegetation structures) in the small-scale observation.

Despite the uncertainties described above, increased levels of the trace elements studied (As, Cd, Cu, Ni, Pb and Sb) were found in mosses between 2015 and 2020. Increasing metal concentrations in mosses for Al, As, Fe, Co, Cr, Hg, Ni, V and Zn are also reported from other EMS participating countries between the Moss Surveys 2015 and 2020, e.g., in Sweden for Al, As, Fe, Co, Cr, Hg, Ni, V and Zn (G. Pihl-Karlsson, pers. comm. Communication, 24.02.2022; Helena Danielsson, e-mail 23.03.2022). Trace elements and nitrogen should remain components of environmental monitoring, as it has been demonstrated that after years of decreasing bioaccumulation, interim trend reversals also occur. In this respect,

the study provides one of many necessary contributions to the discussion on the extent to which analytes of current monitoring programmes are still relevant and up-to-date and whether there are new substances that are also relevant or even more relevant than existing analytes and to what extent this should be taken into account in the design of environmental monitoring.

The increased metal concentrations in mosses over the last five years do not correspond to the corresponding trends in reported metal emissions in Germany (2015–2020; [26]). Rather, there are opposite developments, i.e., while metal emissions are consistently declining, the measured concentrations in the mosses increase between 2015 and 2020. The largest discrepancies are found for Ni. For comparison, France similarly reports an increase in Pb concentrations in mosses between 2015 and 2020, although the trend shown in the French emission inventory is decreasing (Caroline Meyer, e-mail of 20.03.2023). The long-term trends of As, Cd, Cu, Ni and Pb concentrations measured in the mosses, on the other hand, show good overall agreement with the corresponding emission trends in Germany (1990–2020, [26]), although it is noticeable that the long-term trends in the moss data are mostly weaker than in the emission data [12, 13].

Finally, it cannot be assessed whether the significant decreases in metal content in the mosses observed in MM2015 ($n=397$ to 400) or the significant increase observed in MM2020 ($n=26$) each represent exceptions in the long-term trend. This could only be clarified in MM2025 on the basis of a larger sample ($n=400$). A more detailed comparison with the trends in metal accumulation in mosses reported from other European participating countries is also recommended.

This comparison of trends in metal emissions [26] with the values from moss monitoring strongly suggests that it is not sufficient to consider only emission data or the modelled deposition derived from these data. Rather, it is essential to supplement them with technically measured air concentration and atmospheric deposition data. This applies all the more because emission data are usually incomplete and often not based on direct measurements (as in the case of domestic combustion plants), but on semi-quantitative estimates. For an analysis of the temporal trends of atmospheric metal deposition by comparison between technically measured deposition and bioaccumulation measured in mosses, at least 56 sites with distances of less than 5 km between the stations of the air quality monitoring network of the Federal Government/the Länder and the sites of the moss monitoring network sampled since 1990 would be available as a paired sample [27]. An integrative trend analysis based on this would also help

to clarify the question of whether and to what extent the years 2015 or 2020 are to be classified as exceptional years with regard to metal concentrations in the mosses.

The geostatistical area estimates of the MM2020 measurement results can only be seen as an intermediate step towards a more comprehensive campaign in 2025. For this, a measurement network density of at least 350 to 400 sites in Germany is recommended to ensure geostatistical validity according to the results of MM2015 for nitrogen and also all 12 standard elements of the European Moss Survey [2, 28].

Supplementary Information

The online version contains supplementary material available at <https://doi.org/10.1186/s12302-023-00827-z>.

Additional file 1: Figure S1. Geostatistical area estimation of As concentrations in mosses (2020). **Figure S2.** Geostatistical area estimation of Cd concentrations in mosses (2020). **Figure S3.** Geostatistical area estimation of Cu concentrations in mosses (2020). **Figure S4.** Geostatistical area estimation of Ni concentrations in mosses (2020). **Figure S5.** Geostatistical area estimation of Pb concentrations in mosses (2020). **Figure S6.** Geostatistical area estimation of Sb concentrations in mosses (2020).

Author contributions

AD, SN and WS contributed to the study conception and design. The moss specimens were collected by BV. Moss preparation and chemical analyses were performed by AD team. Data collection and analysis were performed by SN. The first draft of the manuscript was written by WS and all authors commented on previous versions of the manuscript. All authors read and approved the final manuscript.

Funding

The study was carried out with own financial resources within the framework of the project "Pilot studies on the suitability of bioindication with mosses for recording the atmospheric deposition of persistent organic pollutants as well as microplastics" funded by the Federal Environment Agency (Departmental research plan 2020, FKz 3720632010, UBA II 4.3). This article belongs to a series of contributions submitted from members of the "Division of Environmental Chemistry and Ecotoxicology" of the "German Chemical Society (GDCh)".

Availability of data and materials

The data sets created and statistically analysed in the current study are to be made available in a suitable repository [NAME] PERSISTENT WEB LINK TO DATASETS].

Declarations

Ethics approval and consent to participate

Not applicable.

Consent for publication

Not applicable.

Competing interests

The authors declare that they have no competing interests.

Received: 17 July 2023 Accepted: 16 December 2023

Published online: 21 February 2024

References

- Harmens H, Foan L, Simon V, Mills G (2013) Terrestrial mosses as biomonitors of atmospheric POPs pollution: a review. *Environ Pollut* 173:245–254
- ICP Vegetation (2020) Heavy metals, nitrogen and POPs in European mosses. Monitoring manual survey 2020. Bangor (United Kingdom) and Dubna (Russian Federation). p 1–27
- Hodson ME (2004) Heavy metals-geochemical bogey men? *Environ Pollut* 129:341–343
- Pourret O, Bollinger J-C, Hursthouse A (2021) Heavy metal: a misused term? *Acta Geochimica* 40:466–471
- Vernon RE (2013) Which elements are metalloids? *J Chem Educ* 90(12):1703–1707
- Herpin U, Lieth H, Markert B (1995) Monitoring of heavy metal pollution in the Federal Republic of Germany with the aid of moss analyses. Berlin: UBA-Texte 31/95
- Siewers U, Herpin U (1998) Heavy metal inputs in Germany. Moss monitoring 1995, Part 1. *Geologisches Jahrbuch, Sonderhefte, Heft SD 2*, Stuttgart: Bornträger
- Siewers U, Herpin U, Straßburger S (2000) Heavy metal inputs in Germany. Moss monitoring 1995, Part 2. *Geologisches Jahrbuch, Sonderhefte, Heft SD 3*, Stuttgart: Bornträger
- Schröder W, Anhelm P, Bau H, Bröcker F, Matter Y, Mitze R, Mohr K, Peichl L, Peiter A, Peronne T, Pesch R, Roostai AH, Roostai Z, Schmidt G, Siewers U (2002) Investigation of pollutant inputs using bioindicators. Analysis and evaluation of the results of moss monitoring 1990, 1995 and 2000. Berlin (Environmental Research Plan of the Federal Minister for the Environment, Nature Conservation and Nuclear Safety. FuE-Project 200 64 218, Final Report, Vols.1–3 + Synthesos Report, commissioned by the Federal Environment Agency), 221 tables, 94 figures. p 29
- Pesch R, Schröder W, Genssler L, Goeritz A, Holy M, Kleppin L, Matter Y (2007) Moss monitoring 2005/2006: *Heavy metals IV* and *total nitrogen*. Berlin (Environmental Research Plan of the Federal Minister for the Environment, Nature Conservation and Nuclear Safety. FuE-Vorhaben 205 64 200, Abschlussbericht, im Auftrag des Umweltbundesamtes). 90 p 11 tabs., 2 figs. (text part); 51 p + 41 maps, 34 tables, 46 diagrams (appendix part)
- Schröder W, Nickel S, Völksen B, Dreyer A, Wosniok W (2019). Use of bioindication methods for the determination and regionalisation of pollutant inputs for an estimation of the atmospheric contribution to current pressures on ecosystems. B1:1–189, Vol. 2:1–296. UBA-Texte 91/2019
- Schröder W, Dreyer A, Nickel S, Völksen B, Wenzel M, Wolf C, Kube C, Türk J (2023) Pilot studies on the suitability of bioindication with mosses for the detection of atmospheric deposition of persistent organic pollutants and microplastics. Research and development project FKZ 3720632010 in the departmental research plan 2020 of the Federal Ministry for the Environment, Nature Conservation, Nuclear Safety and Consumer Protection. Commissioned by the Federal Environment Agency, Dessau. Vols. 1, 2. p 1–138, 1–154
- Schröder W, Nickel S, Dreyer A (2023) Völksen B (2023) Accumulation of atmospheric metals and nitrogen deposition in mosses: temporal development between 1990 and 2020, comparison with emission data and tree canopy drip effects. *Pollutants* 3:89–101
- Steinnes E, Rühling A, Lippo H, Mäkinen A (1997) Reference materials for large-scale metal deposition surveys. *Accred Qual Assur* 2:243–249
- Nickel S, Schröder W, Dreyer A, Völksen B (2023) Mapping spatial and temporal trends of atmospheric deposition of nitrogen at the landscape level in Germany 2005, 2015 and 2020 and their comparison with emission data. *Sci Total Environ* 891(164478):1–7
- Sachs L, Hedderich J (2009) *Angewandte Statistik. Method collection with R [Applied Statistics. Method collection with R]*. Springer, Berlin
- Goovaerts P (1999) Geostatistics in soil science: state-of-the-art and perspectives. *Geoderma* 89(1–2):1–45
- Matheron G (1965) *Regionalised variables and their estimation*. Masson, Paris
- Johnston K, Ver Hoef JM, Krivouchko K, Lucas N (2001) *Using ArcGIS geostatistical analyst*. ESRI Inc., Redlands
- Moran PAP (1950) Notes on continuous stochastic phenomena. *Biometrika* 37(1):17–23
- Isaaks EH, Srivastava RM (1989) *An Introduction to applied geostatistics*. Oxford University Press, New York, p 561
- Olea RA (1999) *Geostatistics for engineers and earth scientists*. Kluwer Academic Publishers, Boston, Dordrecht, London
- Nickel S, Schröder W, Völksen B, Dreyer A (2022) Influence of the canopy drip effect on the accumulation of atmospheric metal and nitrogen deposition in mosses. *Forests* 13(605):1–14
- Wosniok W, Nickel S, Schröder W (2019) R Software tool for calculating minimum Sample Sizes for Arbitrary Distributions (SSAD), Link to scientific software (Version v1). ZENODO. <https://doi.org/10.5281/zenodo.2583010>
- Wosniok W, Nickel S, Schröder W (2020) Development of the software tool Sample Size for Arbitrary Distributions and exemplarily applying it for calculating minimum numbers of moss samples used as accumulation indicators for atmospheric deposition. *Environ Sci Eur* 32(9):1–14
- NaSE (2022) National trend tables for German reporting of atmospheric emissions (heavy metals) 1990–2020, as of August 2022. Federal Environment Agency, Dessau Roßlau
- Nickel S, Schröder W, Ilyin I, Travnikov O (2023) Correlation of modelled atmospheric deposition of cadmium, mercury and lead with the measured enrichment of these elements in moss, vol XVI. Springer, Cham, p 82
- Nickel S, Schröder W (2017) Reorganisation of a long-term monitoring network using moss as biomonitor for atmospheric deposition in Germany. *Ecol Indic* 76:194–206

Publisher's Note

Springer Nature remains neutral with regard to jurisdictional claims in published maps and institutional affiliations.

Submit your manuscript to a SpringerOpen[®] journal and benefit from:

- Convenient online submission
- Rigorous peer review
- Open access: articles freely available online
- High visibility within the field
- Retaining the copyright to your article

Submit your next manuscript at ► [springeropen.com](https://www.springeropen.com)